Quantum-field-theoretic analysis of inflation dynamics in a (2+1)-dimensional universe

M. Samiullah
Department of Physics, Northeast Missouri State University, Kirksville, Missouri 63501-9980

O. Éboli*
Center for Theoretical Physics, Laboratory for Nuclear Science and Department of Physics, Massachusetts Institute of Technology, Cambridge, Massachusetts 02139

So-Young Pi
Department of Physics, Boston University, 590 Commonwealth Avenue, Boston, Massachusetts 02215
(Received 20 May 1991)

We reexamine inflationary scenarios based on slow-rollover transitions, which occur under various initial conditions of the inflation-driving scalar field. We examine inflation dynamics using a recently developed calculational technique for studying a quantum-field-theoretic system in an external environment that is itself changing with time. This method, based on the functional Schrödinger picture, uses a self-consistent Gaussian approximation that, unlike ordinary perturbation theory, reflects some of the nonlinearities of the full quantum theory. Our treatment is confined to planar universes, where the approximation techniques do not suffer from well-known problems associated with scalar field self-interactions in four-dimensional space-time. However, for these toy models we can present concrete and explicit results.

I. INTRODUCTION

Inflationary cosmology [1] attempts to answer some fundamental cosmological questions and, moreover, it provides a possibility of constructing a self-consistent, predictive cosmology. Various inflationary scenarios have been proposed during the last decade to overcome the difficulties in Guth's original model [2], for example, the "new" inflationary scenario [3], "chaotic" inflation [4], and more recently "extended" inflation [5] and its variations. However, so far it seems that none of these models avoid unnatural fine tunings and/or unnatural initial conditions. In this article we reexamine the earlier inflationary scenarios based on "slow-rollover" transitions, such as the "new" and "chaotic" inflation. These models are attractive since the idea behind them is rather simple compared to the more recently proposed "extended" scenarios and therefore deserve further investigation.

The slow-rollover transition was first introduced in the new inflationary scenario [3] to overcome difficulties with the original model [2]. In the new inflationary picture, inflation occurs during a temperature-induced symmetry-breaking phase transition. The scalar field Φ, whose expectation value $\langle\Phi\rangle=\varphi$ plays the role of the order parameter, is initially in thermal equilibrium when the temperature is very high ($T\gg$ critical temperature T_c). The finite-temperature effective potential [6], which describes the energetics of Φ, possesses a global minimum at $\varphi=0$ for $T>T_c$. At zero temperature, however, the potential $V(\varphi)$ has minima at $\varphi=\pm\varphi_c$ and is extremely flat near the maximum at $\varphi=0$ (see Fig. 1). The behavior of the scalar field during the phase transition, based on the static effective potential, is as follows: as the universe cools the scalar field gets caught at $\varphi\approx 0$, in a state called a false vacuum. The energy density of the universe is dominated by the constant vacuum energy density $V(\varphi=0)=\rho_0$ and the universe evolves rapidly into a de Sitter space, which can be described by the metric

$$ds^2=g_{\mu\nu}dx^\mu dx^\nu=dt^2-e^{2\chi t}d\mathbf{x}^2\ , \tag{1.1}$$

where the expansion rate $\chi=\sqrt{(8\pi/3)G_N\rho_0}$ with G_N being Newton's constant. The scalar field hovers for a while at $\varphi\approx 0$, and then eventually begins to roll down the gentle hill of the potential. The inflationary era continues during this slow rollover, since $V(\varphi)$ stays approximately constant for $|\varphi|\ll\varphi_c$.

The most remarkable consequence of the slow-rollover transition is the prediction of density fluctuations [7],

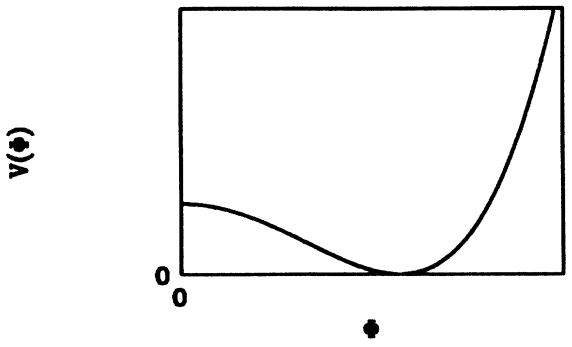

FIG. 1. Typical form of the potential function $V(\phi)$ in the new inflationary scenario.

whose origin is the quantum fluctuations in de Sitter space, occurring during the slow rollover. The predicted density fluctuations must satisfy the upper bound coming from the observed isotropy of the microwave background radiation. This gives a severe constraint on the model: For a scalar field with a double-well potential

$$V(\varphi)=\frac{\lambda}{4}\left[\varphi^2-\frac{\mu^2}{\lambda}\right]^2 \tag{1.2}$$

the upper bound on the self-coupling constant λ is of order 10^{-12}. Furthermore, in order to prevent the self-coupling from becoming large due to radiative corrections, the couplings of Φ to the other fields must be smaller than $\sqrt{\lambda}$. This poses a serious difficulty for the new inflationary scenario: couplings must be fine-tuned and also they are too weak to ensure thermal equilibrium, and thus, thermal equilibrium is only one of many possible initial states.

However, the picture described above is mainly based on restricted analyses, relying on the static, finite-temperature effective potential, which does not properly take into account effects of nonequilibrium dynamics [8]. Moreover, semiclassical [9] or linearized approximations [10] have been frequently made, and the full nonlinearity of an interacting theory is lost. It is conceivable that a more complete analysis may change this picture, permitting moderate values for the scalar self-coupling λ [8]. This could allow the thermal-equilibrium initial state to be a viable starting point, which is quite natural in the context of the hot big-bang cosmology. In fact, the analysis carried out in Ref. [11], taking into account some of the nonequilibrium and nonlinear effects, presents a picture that is quite different from the standard new inflationary scenario.

The chaotic inflationary model [4] was introduced to avoid the difficulty with the initial condition in the new inflationary model. Here, the inflation-driving field's initial state is not in thermal equilibrium with the thermal bath. It starts out in a configuration with a spatially homogeneous large value of φ. [The potential function need not be a double well: it may be of the form described by Eq. (1.2) with $\mu^2\leq 0,\lambda>0$ or $\mu^2>0,\lambda=0$.]

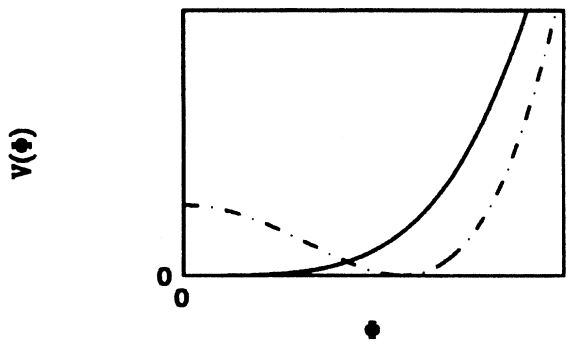

FIG. 2. Two types of potential function $V(\phi)$ in the chaotic inflationary scenario.

Then, initially the energy density of the scalar field is much larger than the radiation energy and inflation occurs while φ rolls down the hill from the large initial value toward the global minimum at $\varphi_c=0$ or $\varphi_c=\pm\mu/\sqrt{\lambda}$, depending on the value of the parameters (see Fig. 2). However, such an initial state is also only one of many possible initial configurations and it is as unnatural as the thermal equilibrium initial configuration in the new inflationary model, if the self-coupling λ is indeed small.

In order to survey possibilities of inflation, we need to consider initial conditions that are more general than thermal equilibrium or the arbitrarily chosen chaotic configuration.

According to various classical analyses [9], there are more general initial conditions on Φ for which the Universe evolves into an inflationary phase by first dynamically achieving the homogeneous configuration where $\varphi=0$, as in the new inflation (Fig. 1) or as in chaotic inflation (Fig. 2). However, the physical significance of the classical function $\varphi_{\rm cl}(\mathbf{x},t)$ is not at all clear. Especially for the case where $\varphi_{\rm cl}$ rolls down from the maximum of the potential at $\varphi=0$, the quantum-mechanical expectation value $\langle\Phi(\mathbf{x},t)\rangle$ remains zero for all time. In fact, as pointed out in Ref. [10], the quantum fluctuations govern the dynamics of the early stage of the slow rollover, and classical behavior appears only in the late time.

The purpose of this article is to study the onset of inflation by analyzing the quantum-mechanical time evolution of the inflation-driving scalar field for various initial conditions, including thermal equilibrium. We use a recently developed calculational technique for studying a quantum-field-theoretic system in an external environment that is changing with time [12]. This technique is based on the functional Schrödinger picture where mixed states are described by a functional density matrix and the fundamental dynamical equation is the Liouville–von Neumann equation. This equation cannot be solved for nonlinear (interacting) systems. In Ref. [12], an approximation scheme was developed based on a variational principle whose exact implementation leads to the (intractable) Liouville–von Neumann equation. By taking a Gaussian ansatz for the density matrix, one obtains approximate but tractable equations for the parameters which define the ansatz. This method is a self-consistent approximation that, unlike the ordinary perturbation theory, reflects some of the nonlinearities of the full quantum theory.

The equations that we deal with are the analogues of time-dependent Hartree–Fock equations or large-N approximations. As such, they suffer from well-known shortcomings, especially in higher-dimensional field theory [13]. Therefore we study the self-interacting scalar field in three-dimensional space-time. For a given initial state (pure or mixed) the onset of inflation is studied numerically by solving the coupled semiclassical Einstein and matter equations, where the matter equations are given by the Gaussian approximation.

This article is organized as follows: In Sec. II we describe the model used for the early Universe and also our method of calculation. Section III contains the descrip-

tion of our code used for solving the time-evolution equations. We present our numerical results in Sec. IV, and in Sec. V we compare our results with those obtained in the linearized approximation [10] and in the large-N approximation [11].

II. MODEL FOR THE EARLY UNIVERSE AND METHOD OF CALCULATION

In this section we describe our model for the early Universe and discuss the calculational techniques that we employ, including some theoretical issues such as renormalization.

A. Model for the early Universe

In our model, the matter content of the Universe consists of two parts: the first is a self-interacting scalar field, while the second comprises the remaining matter and radiation, which provides the environment, in thermal equilibrium. We assume that the interactions between the two systems are negligible and their time evolutions are adiabatic: entropy in each system is conserved separately.

We consider a self-interacting scalar field in a $(2+1)$-dimensional flat Robertson–Walker space-time with the line element

$$ds^2=dt^2-a^2(t)\,d\mathbf{x}^2 , \tag{2.1}$$

where $a(t)$ is the scale factor describing the dynamics of the universe. For a given scale factor $a(t)$, the scalar field dynamics is assumed to be governed by the action

$$I=\int d^3x\,\mathcal{L}=\int d^2\mathbf{x}\,dt\sqrt{-g}\left[\tfrac{1}{2}g^{\mu\nu}\partial_\mu\Phi\partial_\nu\Phi-\tfrac{1}{2}(\mu^2+\xi R)\Phi^2-\frac{\lambda}{4!}\Phi^4\right] , \tag{2.2}$$

where ξ is the coupling between the scalar field and the Ricci scalar $R=2(\dot a/a)^2+4(\ddot a/a)$ of the background metric and it takes the value $\xi=\xi_{\rm cc}\equiv\frac{1}{8}$, for the conformally coupled field, and $\xi=0$, for the case of minimal coupling.

The behavior of the classical function $a(t)$ is assumed to be described by the semiclassical Einstein equation

$$G_{\mu\nu}=R_{\mu\nu}-\tfrac{1}{2}g_{\mu\nu}R=-8\pi G\langle T_{\mu\nu}\rangle , \tag{2.3}$$

where $G_{\mu\nu}$ is the Einstein tensor and $\langle T_{\mu\nu}\rangle$ is the expectation value of the energy-momentum tensor of the total matter fields in the quantum state we are considering. In our model $\langle T_{\mu\nu}\rangle$ may be written in terms of two parts:

$$\langle T_{\mu\nu}\rangle=\langle T_{\mu\nu}(\Phi)\rangle+\langle T_{\mu\nu}\rangle_{\rm rad} , \tag{2.4}$$

where $\langle T_{\mu\nu}(\Phi)\rangle$ is the expectation value of the scalar field energy-momentum tensor in the quantum state whose time evolution is being studied, and $\langle T_{\mu\nu}\rangle_{\rm rad}$ is the contribution from matter and radiation in thermal equilibrium. With the metric (2.1), $\langle T_{\mu\nu}\rangle$ is diagonal for translationally invariant field configurations:

$$\langle T_{\mu\nu}\rangle=\mathrm{diag}(\langle\epsilon\rangle,\ \langle p\rangle a^2,\ \langle p\rangle a^2) , \tag{2.5}$$

where $\langle\epsilon\rangle$ and $\langle p\rangle$ are the average energy density and pressure, respectively, and, therefore, the Einstein equation reduces to

$$H^2\equiv\left[\frac{\dot a}{a}\right]^2=8\pi G_N[\langle T_{00}(\Phi)\rangle+\langle T_{00}\rangle_{\rm rad}] . \tag{2.6}$$

In $(2+1)$-dimensional space-time $\langle T_{00}\rangle_{\rm rad}$ is given by

$$\langle T_{00}\rangle_{\rm rad}=nT^3 ,\qquad n=\frac{\zeta(3)(g_B+\frac{3}{4}g_F)}{\pi} , \tag{2.7}$$

where $g_B(g_F)$ is the number of bosonic (fermionic) degrees of freedom and ζ is the Riemann zeta function. From our assumption of adiabatic time evolution of each system, the temperature of radiation changes with time as $1/a(t)$ and may be parametrized as

$$T(t)=\frac{a(t_0)}{a(t)}T(t_0) , \tag{2.8}$$

where t_0 is some given initial time.

Hence, for a given initial state of the universe, the time evolution of Φ and $a(t)$ will be self-consistently determined by the coupled equations

$$\left[\frac{\dot a}{a}\right]^2=8\pi G_N(\langle T_{00}(\Phi)\rangle+nT^3) ,\qquad \text{dynamical equation for } \Phi . \tag{2.9}$$

B. Functional Schrödinger picture: Gaussian variational approximation

We now discuss the technique that provides a concrete dynamical equation, which governs the time evolution of Φ from a given initial state.

Our calculational technique is based on the functional Schrödinger picture [14]. The time evolution of a system from a definite initial configuration is efficiently accomplished in a Schrödinger picture description where the initial data consist of specifying a pure or mixed state.

In the field-theoretic Schrödinger picture, states are described by wave functionals $\Psi(\phi)$ of a c-number field $\phi(\mathbf{x})$ at a fixed time. The inner product is defined by functional integration,

$$\langle\Psi_1|\Psi_2\rangle\Longleftrightarrow\int D\phi\,\Psi_1^*(\phi)\Psi_2(\phi) , \tag{2.10}$$

while operators are represented by functional kernels:

$$\mathcal{O}|\Psi\rangle\Longleftrightarrow\int D\phi'\mathcal{O}(\phi,\phi')\Psi(\phi') . \tag{2.11}$$

For the canonical field operator at a fixed time $\Phi(\mathbf{x})$ (the time argument is common to all operators in the Schrödinger picture, so it is suppressed), we use a diago-

nal kernel, $\Phi(\mathbf{x}) \Longleftrightarrow \phi(\mathbf{x})\delta(\phi-\phi')$; the canonical commutation relations determine the canonical momentum kernel, $\Pi(\mathbf{x}) \Longleftrightarrow -i[\delta/\delta\phi(\mathbf{x})]\delta(\phi-\phi')$. Both kernels involve a functional δ function. Hence Φ acts by multiplication on functionals of ϕ, while Π acts by functional differentiation. In this way, the action of any operator constructed from Φ and Π is

$$\mathcal{O}(\Pi,\Phi)|\Psi\rangle \Longleftrightarrow \mathcal{O}\left[-i\frac{\delta}{\delta\phi},\ \phi\right]\Psi(\phi)\ . \tag{2.12}$$

The fundamental dynamical equation is the time-dependent functional Schrödinger equation for a time-dependent wave functional $\Psi(\phi,t)$. The equation takes a definite form once a Hamiltonian operator $\mathcal{H}(\Pi,\Phi)$ is specified:

$$i\frac{\partial\Psi}{\partial t}=\mathcal{H}\left[-i\frac{\delta}{\delta\phi},\phi\right]\Psi\ . \tag{2.13}$$

When the initial state of a system is a pure state, described by a wave functional Ψ, Eq. (2.13) determines uniquely subsequent evolution.

In the Schrödinger picture for field theory, a mixed state is described by a functional density matrix [12]

$$\begin{aligned}&\rho(\phi_1,\phi_2)=\sum_n p_n\Psi_n(\phi_1)\Psi_n^*(\phi_2)\ ,\\ &\mathrm{Tr}\rho=\int D\phi\,\rho(\phi,\phi)=1\ ,\end{aligned} \tag{2.14}$$

where $\{\Psi_n\}$ is a complete set of wave functionals and p_n is the probability that the system is in state n. The average value of physical quantities described by operators $\mathcal{O}$, which in turn are represented by kernels $\mathcal{O}(\phi_1,\phi_2)$, are determined by the density matrix

$$\langle\mathcal{O}\rangle=\mathrm{Tr}\rho\mathcal{O}=\int D\phi_1 D\phi_2\rho(\phi_1,\phi_2)\mathcal{O}(\phi_2,\phi_1)\ . \tag{2.15}$$

The entropy of a system described by the density matrix (2.14) is

$$S=-k_B\mathrm{Tr}\rho\ln\rho=-k_B\sum_n p_n\ln p_n\ , \tag{2.16}$$

with k_B the Boltzmann constant. In thermal equilibrium, the p_n's are Boltzmann distributed; i.e., they are given by e^{-E_n/k_BT}, where E_n is the energy eigenvalue of the state Ψ_n. In general, for nonstatic situations the p_n's need not be the Boltzmann distribution, and can also change in time.

If we assume that Ψ_n is governed by the time-dependent Schrödinger equation, the time variation of the density matrix is given by

$$\frac{d\rho}{dt}=i[\rho,\mathcal{H}]+\sum_n\frac{dp_n}{dt}\Psi_n(\phi_1)\Psi_n^*(\phi_2)\ , \tag{2.17}$$

where $\mathcal{H}$ is some time-dependent Hamiltonian.

For a given Hamiltonian and initial condition, Eq. (2.17), unlike the Schrödinger equation, requires additional information in order to determine subsequent evolution: (dp_n/dt) must be given. We have already assumed in our model that the entropy of the scalar field is conserved. In view of (2.16) it is simplest to assume that the entropy conservation holds because the occupation probabilities are constant: $(dp_n/dt)=0$. Then the isoentropic time evolution of the density matrix is governed by the Liouville–von Neumann equation

$$\frac{d\rho}{dt}=i[\rho,\mathcal{H}]\ , \tag{2.18}$$

The time-dependent functional Schrödinger equation (2.13) and the Liouville–von Neumann equation (2.18) are not directly integrable, except for linear problems described by a quadratic Hamiltonian. To obtain a solution for our system we use an approximation in which variational principles, leading to Eqs. (2.13) and (2.18), are implemented approximately.

The time-dependent variational principle that yields the time-dependent Schrödinger equation is due to Dirac [15]: one defines the effective action Γ as the time integral of the diagonal matrix element of $i\partial_t-\mathcal{H}$,

$$\Gamma=\int dt\,\langle\Psi|i\partial_t-\mathcal{H}|\Psi\rangle\ , \tag{2.19}$$

and demand that Γ be stationary against arbitrary variations of $|\Psi\rangle$ and $\langle\Psi|$ with appropriate boundary conditions. This results in the time-dependent Schrödinger equation.

In the variational principle that gives the Liouville–von Neumann equation [12,16] one considers a nonequilibrium effective action Γ given by

$$\Gamma=-\int_{t_i}^{t_f}dt\ \mathrm{Tr}\left[\rho\left[\frac{d\Lambda}{dt}+i[\mathcal{H},\Lambda]\right]\right]-\mathrm{Tr}(\rho\Lambda)|_{t=t_f}\ . \tag{2.20}$$

Here Λ, ρ, and $\mathcal{H}$ are time-dependent functional kernels and the trace is over these kernels. We impose the boundary conditions that $\Lambda|_{t=t_f}=1$ and $\rho|_{t=t_i}=\rho_0$, where ρ_0 is some given initial density matrix. Demanding that Γ is stationary against variations of ρ and Λ leads to the Liouville–von Neumann equation for ρ and an equation for Λ. The variable Λ plays the role of a Lagrange multiplier, and it is also needed to give our action a canonical structure, which requires a pair of variables, i.e., in a sense ρ and Λ form a canonically conjugate pair. The boundary condition $\Lambda|_{t=t_f}=1$ selects the solution $\Lambda=1$ for all time and we are left with a variational formulation of the Liouville–von Neumann equation.

Applying the variational principles in (2.19) and (2.20) with a restricted variational ansatz, in the Rayleigh–Ritz manner, one obtains approximate but tractable equations describing the time evolution of a nonlinear system for a given initial pure and mixed state, respectively. For the evolution of a pure state, a variational approximation in which a Gaussian ansatz is taken for the wave functional has been developed in Ref. [17]. More recently, a similar approximation for studying mixed-state time evolution has been formulated in Ref. [12], by taking a Gaussian ansatz for the density matrix and implementing the variational principle (2.20). In this article we shall apply this technique. The variational equations obtained in this approximation are similar to the time-dependent Hartree–Fock equations or large-N approximations and for a pure state they reduce to the approximate equations obtained in Ref. [17] using Dirac's variational principle.

The most general Gaussian ansatz for the density matrix is given by

$$\rho(\phi_1,\phi_2)=N_\delta \exp\left[i\int_{\mathbf{x}}\pi(\mathbf{x},t)[\phi_1(\mathbf{x})-\phi_2(\mathbf{x})]\right]$$
$$\times\exp\left[-\int_{\mathbf{x},\mathbf{y}}\{[\phi_1(\mathbf{x})-\varphi(\mathbf{x},t)][\tfrac{1}{4}G_\delta^{-1}(\mathbf{x},\mathbf{y},t)-i\Sigma_\delta(\mathbf{x},\mathbf{y},t)][\phi_1(\mathbf{y})-\varphi(\mathbf{y},t)]\right.$$
$$+[\phi_2(\mathbf{x})-\varphi(\mathbf{x},t)][\tfrac{1}{4}G_\delta^{-1}(\mathbf{x},\mathbf{y},t)+i\Sigma_\delta(\mathbf{x},\mathbf{y},t)][\phi_2(\mathbf{y})-\varphi(\mathbf{y},t)]$$
$$\left.+[\phi_1(\mathbf{x})-\varphi(\mathbf{x},t)](G_\delta^{-1/2}\delta G_\delta^{-1/2})(\mathbf{x},\mathbf{y},t)[\phi_2(\mathbf{y})-\varphi(\mathbf{y},t)]\}\right]. \tag{2.21}$$

N_δ is a real, time-dependent normalization factor which ensures $\mathrm{tr}\rho=1$. G_δ, Σ_δ, and δ are real kernels satisfying the Hermiticity condition $\rho(\phi_1,\phi_2)=\rho^*(\phi_2,\phi_1)$. The variational parameters are $\varphi,\pi,G_\delta,\Sigma_\delta,\delta$, and N_δ. Let us observe that a nonvanishing δ is a measure of the amount by which the density matrix differs from a pure state, and is related to the occupation probabilities p_n in Eq. (2.14). For $\delta=0$, ρ describes a pure state since it can be cast into the form $\rho(\phi_1,\phi_2)=\Psi(\phi_1)\Psi^*(\phi_2)$, with Ψ being a Gaussian wave functional.

With the above density matrix, the linear averages are given by

$$\langle\Phi(\mathbf{x})\rangle=\varphi(\mathbf{x},t)\ , \tag{2.22a}$$
$$\langle\Pi(\mathbf{x})\rangle=\pi(\mathbf{x},t)\ , \tag{2.22b}$$

while bilinear averages are

$$\langle\Phi(\mathbf{x})\Phi(\mathbf{y})\rangle=\varphi(\mathbf{x},t)\varphi(\mathbf{y},t)+[G_\delta^{1/2}(1-\delta)^{-1}G_\delta^{1/2}](\mathbf{x},\mathbf{y},t)\ , \tag{2.22c}$$

$$\langle\Pi(\mathbf{x})\Pi(\mathbf{y})\rangle=\pi(\mathbf{x},t)\pi(\mathbf{y},t)+\tfrac{1}{4}[G_\delta^{-1/2}(1+\delta)G_\delta^{-1/2}](\mathbf{x},\mathbf{y},t)+4[\Sigma_\delta G_\delta^{1/2}(1-\delta)^{-1}G_\delta^{1/2}\Sigma_\delta](\mathbf{x},\mathbf{y},t)\ , \tag{2.22d}$$

$$\langle\Phi(\mathbf{x})\Pi(\mathbf{y})\rangle=\frac{i}{2}\delta(\mathbf{x}-\mathbf{y})+2[G_\delta^{1/2}(1-\delta)^{-1}G_\delta^{1/2}\Sigma_\delta](\mathbf{x},\mathbf{y},t)\ . \tag{2.22e}$$

As can be seen in Eqs. (2.22a) and (2.22b), the Gaussian density matrix ρ describes, in general, a state with an inhomogeneous field configuration. In this article, for simplicity, we shall consider states with homogeneous field configurations which are consistent with our approximation that the background metric is a perfect Robertson–Walker space-time. Then the kernels G_δ,Σ_δ, and δ are diagonalized in momentum space.

To implement the variational principle we also need an ansatz for Λ with the same number of variational parameters as in ρ. By choosing an appropriate ansatz for Λ and varying the effective action (2.20) with the respect to the parameters in Λ we obtain the dynamical equations for the parameters which define ρ in (2.21) [12]. For our system described by the action (2.2), the variational equations of motion are

$$\dot\varphi=a^{-2}\pi\ , \tag{2.23a}$$
$$\dot\pi=-a^{-2}\left[m_\delta^2(t)+\xi_{\mathrm{cc}}R-\frac{\lambda}{3}\varphi^2\right]\varphi\ , \tag{2.23b}$$
$$\dot G_\delta(\mathbf{k})=4a^{-2}\Sigma_\delta(\mathbf{k})G_\delta(\mathbf{k})\ , \tag{2.23c}$$
$$\dot\Sigma_\delta(\mathbf{k})=\tfrac{1}{8}a^{-2}G_\delta^{-2}(\mathbf{k})[1-\delta^2(\mathbf{k})]-2a^{-2}\Sigma_\delta^2(\mathbf{k})-\tfrac{1}{2}a^2[\mathbf{k}^2a^{-2}+m_\delta^2(t)+\xi_{\mathrm{cc}}R]\ , \tag{2.23d}$$
$$\dot\delta(\mathbf{k})=0\ , \tag{2.23e}$$

where

$$m_\delta^2(t)=\mu^2+(\xi-\xi_{\mathrm{cc}})R+\frac{\lambda}{2}\varphi^2+\frac{\lambda}{2}\int_{\mathbf{k}}\frac{G_\delta}{1-\delta}\ , \tag{2.23f}$$

and the Fourier transforms are defined by $f(\mathbf{x},\mathbf{y})=\int_{\mathbf{k}}e^{-i\mathbf{k}\cdot(\mathbf{x}-\mathbf{y})}f(\mathbf{k})$ with $\int_{\mathbf{k}}$ representing $\int[d^2\mathbf{k}/(2\pi)^2]$. The constant $\xi_{\mathrm{cc}}=\frac{1}{8}$ has been introduced in Eqs. (2.23a)–(2.23f) for calculational convenience.

To apply these equations, first we must choose our vacuum state, which is not unique in quantum field theory in a time-dependent metric [18], and then study the ultraviolet divergences. To do so, it is convenient to obtain a second-order differential equation for G_δ by eliminating Σ_δ, using (2.23c):

$$\ddot G_\delta=\tfrac{1}{2}a^{-4}(1-\delta^2)G_\delta^{-1}+\tfrac{1}{2}G_\delta^{-1}\dot G_\delta^2-2H\dot G_\delta-2[k^2a^{-2}+m_\delta^2(t)+\xi_{\mathrm{cc}}R]G_\delta\ . \tag{2.24}$$

[We shall use $k=|\mathbf{k}|$, since G_δ depends only on the magnitude of $\mathbf{k}$.] Next, by defining

$$G_\delta=G\sqrt{1-\delta^2} \tag{2.25}$$

we obtain an equation for G:

$$\ddot G=\tfrac{1}{2}a^{-4}G^{-1}+\tfrac{1}{2}G^{-1}\dot G^2-2H\dot G-2[k^2a^{-2}+m_\delta^2(t)+\xi_{\mathrm{cc}}R]G\ , \tag{2.26a}$$

where

$$m_\delta^2(t)=\mu^2+(\xi-\xi_{\mathrm{cc}})R+\frac{\lambda}{2}\varphi^2+\frac{\lambda}{2}\int_{\mathbf{k}}G\left[\frac{1+\delta}{1-\delta}\right]^{1/2}. \tag{2.26b}$$

We observe that (2.26a) has exactly the same form as the one for a pure state, obtained from (2.23) by setting $\delta=0$, except that the effective mass in (2.26b) contains a δ dependence. For the thermal equilibrium configuration,

G is of the same form as the vacuum solution and $\delta(k)$ is associated with the Boltzmann distribution.

We shall choose as our vacuum the conventional adiabatic vacuum [18], which behaves as the Minkowski vacuum in the limit when the expansion rate of the universe is much smaller than the effective frequency. The vacuum solution [19] in the Gaussian approximation is then, for large k,

$$G(k)=\frac{1}{2a\sqrt{k^2+m^2(t)a^2}}[1+O(|ka^{-1}|^{-3})] , \quad (2.27)$$

where $m^2(t)=m_\delta^2(t)|_{\delta=0}$ evaluated at $\varphi_{\min}$, which is the minimum of the effective potential. This introduces to the effective mass of (2.23f) and (2.26b) a divergence of the form, for $\delta=0$,

$$D=\frac{\lambda}{2}\int_k \frac{1}{2a\sqrt{k^2+m^2(t)a^2}} =\frac{\lambda}{2}\int_k \left[\frac{1}{2a|k|}-\frac{m^2(t)a}{4|k|^3}+\cdots\right] . \quad (2.28)$$

Therefore the variational equations are not well defined and require renormalization. The most convenient way to regularize a quantum field theory in curved space-time is to use dimensional regularization [20], which preserves the general covariance. Dimensional regularization may be applied to the functional Schrödinger picture by analytically continuing only the spatial dimension, and it has been used in Ref. [19] to renormalize the self-interacting scalar field in $n=(3+1)$-dimensional Robertson-Walker metric.

In dimensional regularization, the first term in the second integral in (2.28) is simply zero [20] and the second term is proportional to the gamma function $\Gamma(n-4)$. Therefore, in $3+1$ dimensions only the logarithmic divergence appears as a pole in the gamma function and it can be removed by renormalizing the mass μ and coupling constants λ and ξ. On the other hand, the theory does not require renormalization in $n=2+1$ dimensions. However, in order to perform the numerical calculation, we must use the cutoff procedure. In the $(n=2+1)$-dimensional space-time that we are considering the first term in the second integral in (2.28) is divergent and cutoff dependent and it can be eliminated by a mass renormalization:

$$\lambda_R=\lambda ,$$
$$\xi_R=\xi , \quad (2.29a)$$
$$\mu_R^2=\mu^2-\frac{\lambda}{2}I ,$$

where

$$I=\int_k \frac{1}{2a|k|} . \quad (2.29b)$$

The prescription (2.29) renders the effective mass $m^2(t)$ finite in the vacuum sector:

$$m^2(t)=\mu_R^2+(\xi_R-\xi_{cc})R+\frac{\lambda_R}{2}\varphi^2 +\frac{\lambda_R}{2}\int_k\left[G-\frac{1}{2a|k|}\right] . \quad (2.30)$$

For mixed states, i.e., for $\delta(k)\neq 0$, it is straightforward to see that the effective mass $m_\delta^2(t)$ in (2.26b) is rendered finite by the vacuum renormalization provided the large-k behavior of $G(k)$ is given by in (2.27) and $\delta(k)$ vanishes sufficiently fast $[O(|k|^{-3})]$. This is the case, for example, when the system is in thermal equilibrium where $\delta(k)$ vanishes exponentially for $|\mathbf{k}|\gg T$:

$$m_\delta^2(t)=\mu_R^2+(\xi_R-\xi_{cc})R+\frac{\lambda_R}{2}\varphi^2 +\frac{\lambda_R}{2}\int_k\left[G\left[\frac{1+\delta}{1-\delta}\right]^{1/2}-\frac{1}{2a|k|}\right] . \quad (2.31)$$

It must be emphasized that this renormalization prescription works only for states that exhibit the high-k behavior given by (2.27) (these are the states which possess a finite particle number density with respect to the chosen vacuum [19]). In the initial-value problem, this implies that the initial conditions $G_\delta(k,t_0)$ and $\dot{G}_\delta(k,t_0)$ at some initial time t_0 must have the large-k behavior [19]

$$G_\delta(k,t_0)=\frac{1}{2a(t_0)\sqrt{k^2+m_\delta^2(t_0)a^2(t_0)}}[1+O(|k|^{-3})] ,$$
$$\dot{G}_\delta(k,t_0)=[O(|k|^{-2}) \text{ or smaller}] , \quad (2.32)$$

where $m_\delta^2(t_0)$ is the self-consistently determined initial mass defined as in (2.31).

C. Finite renormalized semiclassical Einstein equation

Now the coupled Einstein-matter equations in (2.9) have a specific form:

$$\left[\frac{\dot{a}}{a}\right]^2=8\pi G_N(\langle T_{00}(\Phi)\rangle+nT^3) ,$$
Eqs. (2.23a)–(2.23e) with m_δ^2 given in (2.31) , (2.33)

where the expectation value of the energy-momentum tensor is taken in the Gaussian state (2.21).

In $(n=3+1)$-dimensional space-time Eq. (2.33) is somewhat inconsistent in that quantum effects of matter are included, but quantum gravity effects are ignored. From the theoretical point of view, such semiclassical approximation is often justified by the renormalizability of $\langle T_{\mu\nu}(\Phi)\rangle$, which contains infinities, even in the free theory, arising due to the short-distance behavior of $\langle\Phi^2(\mathbf{x})\rangle$. However, in $(n=2+1)$-dimensional space-time there are no propagating gravitons; consequently (2.33) is a consistent approximation.

We shall discuss how we take care of infinities in $\langle T_{\mu\nu}(\Phi)\rangle$ in our numerical calculation. The energy-momentum tensor for the scalar field described by the action (2.2) is

$$T_{\mu\nu}=\frac{2}{\sqrt{-g}}\frac{\delta I}{\delta g^{\mu\nu}}$$
$$=\partial_\mu\Phi\partial_\nu\Phi-g_{\mu\nu}[\tfrac{1}{2}g^{\alpha\beta}\partial_\alpha\Phi\partial_\beta\Phi-V(\Phi)]$$
$$-\xi(G_{\mu\nu}\Phi^2-g_{\mu\nu}g^{\alpha\beta}\Phi^2_{;\alpha;\beta}+\Phi^2_{;\mu;\nu}) , \quad (2.34)$$

where the notation $;\mu$ denotes the covariant derivative with respect to the space-time index μ, and $V(\Phi)=\frac{1}{2}\mu^2\Phi^2+(\lambda/4!)\Phi^4$. [$T_{\mu\nu}$ in (2.34), which is the source of the Einstein equation, does not coincide, for $\xi\neq 0$, with the canonical energy-momentum tensor $T^c_{\mu\nu}=\partial_\mu\Phi\partial_\nu\Phi-g_{\mu\nu}\mathcal{L}$.]

In the flat Robertson–Walker metric of (2.1), the expectation value of $T_{\mu\nu}$ in the translationally invariant Gaussian state of (2.21) has the form

$$\langle T_{00}\rangle=\tfrac{1}{2}a^{-4}\pi^2+V(\varphi)-\xi(G_{00}\varphi^2-4a^{-2}H\varphi\pi)$$
$$+\tfrac{1}{8}a^{-4}[G_\delta^{-1/2}(1+\delta)G_\delta^{-1/2}](\mathbf{x},\mathbf{x},t)+2a^{-4}[\Sigma_\delta G_\delta^{1/2}(1-\delta)^{-1}G_\delta^{1/2}\Sigma_\delta](\mathbf{x},\mathbf{x},t)$$
$$+\tfrac{1}{2}\{(-a^{-2}\nabla_x^2+\mu^2)[G_\delta^{1/2}(1-\delta)^{-1}G_\delta^{1/2}](\mathbf{x},\mathbf{y},t)\}|_{\mathbf{x}=\mathbf{y}}$$
$$-\xi\{G_{00}[G_\delta^{1/2}(1-\delta)^{-1}G_\delta^{1/2}](\mathbf{x},\mathbf{x},t)-8Ha^{-2}[\Sigma_\delta G_\delta^{1/2}(1-\delta)^{-1}G_\delta^{1/2}](\mathbf{x},\mathbf{x},t)\}$$
$$-\frac{\lambda}{8}[G_\delta^{1/2}(1-\delta)^{-1}G_\delta^{1/2}](\mathbf{x},\mathbf{x},t)[G_\delta^{1/2}(1-\delta)^{-1}G_\delta^{1/2}](\mathbf{x},\mathbf{x},t) , \quad (2.35a)$$

$$\langle T_{ij}\rangle=a^2\delta_{ij}\Bigg[\tfrac{1}{2}a^{-4}\pi^2-V(\varphi)-\xi(a^{-2}\tfrac{1}{2}\delta^{nm}G_{nm}\varphi^2+2a^{-2}H\varphi\pi+\partial_t^2\varphi^2)$$
$$+\tfrac{1}{8}a^{-4}[G_\delta^{-1/2}(1+\delta)G_\delta^{-1/2}](\mathbf{x},\mathbf{x},t)+2a^{-4}[\Sigma_\delta G_\delta^{1/2}(1-\delta)^{-1}G_\delta^{1/2}\Sigma_\delta](\mathbf{x},\mathbf{x},t)$$
$$-\tfrac{1}{2}[\mu^2-(\xi-\xi_{cc})R][G_\delta^{1/2}(1-\delta)^{-1}G_\delta^{1/2}](\mathbf{x},\mathbf{x},t)$$
$$-\xi\Bigg[\frac{a^{-2}}{2}\delta^{nm}G_{nm}[G_\delta^{1/2}(1-\delta)^{-1}G_\delta^{1/2}](\mathbf{x},\mathbf{x},t)+4a^{-2}H[\Sigma_\delta G_\delta^{1/2}(1-\delta)^{-1}G_\delta^{1/2}](\mathbf{x},\mathbf{x},t)$$
$$+\partial_t^2[G_\delta^{1/2}(1-\delta)^{-1}G_\delta^{1/2}](\mathbf{x},\mathbf{x},t)\Bigg]$$
$$+\frac{\lambda}{8}[G_\delta^{1/2}(1-\delta)^{-1}G_\delta^{1/2}](\mathbf{x},\mathbf{x},t)[G_\delta^{1/2}(1-\delta)^{-1}G_\delta^{1/2}](\mathbf{x},\mathbf{x},t)\Bigg] , \quad (2.35b)$$

$$\langle T_{0i}\rangle=0 . \quad (2.35c)$$

As can be seen from the above expression $\langle T_{\mu\nu}\rangle$ may be divergent due to infinities contained in $G_\delta(\mathbf{x},\mathbf{x})$. The finite, renormalized energy-momentum tensor is defined by subtracting the divergent part of $\langle T_{\mu\nu}\rangle$:

$$\langle T_{\mu\nu}\rangle_{\text{ren}}\equiv\langle T_{\mu\nu}\rangle-\langle T_{\mu\nu}\rangle_{\text{sub}} . \quad (2.36)$$

To define the subtraction $\langle T_{\mu\nu}\rangle_{\text{sub}}$, first one must regularize the theory in such a way that general covariance is preserved. One well-known procedure is to use dimensional regularization, which we have discussed above. In Ref. [19], $\langle T_{\mu\nu}\rangle$ has been evaluated in $(n=d+1)$-dimensional space-time: possible logarithmic divergences appear as poles in the gamma functions $\Gamma(n-4)$ and $\Gamma(n-2)$, but all other divergent integrals vanish. When $\langle T_{\mu\nu}\rangle$ is divergent, as in $n=4$ dimensions, for example, the subtraction $\langle T_{\mu\nu}\rangle_{\text{sub}}$ must be expressed in terms of covariantly conserved geometrical tensors so that they can be absorbed by renormalization of the coupling constants in the generalized Einstein equation. Moreover, there is a further subtlety in defining the finite part of the subtraction [18]. None of this need concern us because at $n=3$ $\langle T_{\mu\nu}\rangle$ is simply finite and no subtraction is required.

However, in our numerical calculation, where the cutoff procedure is used, the integrals, which vanish in dimensional regularization, remain divergent. By using the cutoff procedure, we need not only mass renormalization, as we have shown, but also $\langle T_{\mu\nu}\rangle$ needs subtraction. Moreover, introducing a cutoff breaks the covariance of the theory. Therefore, we shall use the result of dimensional regularization, in which all the divergent integrals vanish in $n=3$ dimensions, as a guidance in defining the finite $\langle T_{\mu\nu}\rangle$ so that the $\langle T_{\mu\nu}\rangle$ is covariantly conserved.

First, we renormalize the mass according to Eq. (2.29), and then evaluate the divergent part of $\langle T_{\mu\nu}\rangle$ using the large-$\mathbf{k}$ behavior of $G(\mathbf{k},t)$ in (2.27):

$$\langle T_{00}\rangle_{\text{sub}}=-\frac{\lambda_R}{8}\left[\int_{\mathbf{k}}^{\Lambda}\frac{1}{2a|\mathbf{k}|}\right]^2+\frac{1}{2a^3}\int_{\mathbf{k}}^{\Lambda}|\mathbf{k}|+\int_{\mathbf{k}}^{\Lambda}\frac{1}{2a|\mathbf{k}|}\left[\frac{\mu_R^2}{2}+\frac{\xi_R-\xi_{cc}}{2}R-(\xi_R-\xi_{cc})(4H^2+2\dot{H})\right] , \quad (2.37)$$

$$\langle T_{ij}\rangle_{\rm sub}=a^2\delta_{ij}\left[\frac{\lambda_R}{8}\left[\int_{\rm k}^{\Lambda}\frac{1}{2a|\mathbf{k}|}\right]^2+\frac{1}{4a^3}\int_{\rm k}^{\Lambda}|\mathbf{k}|+\int_{\rm k}^{\Lambda}\frac{1}{2a|\mathbf{k}|}\left[\frac{m_\delta^2(t)}{4}-\frac{\mu_R^2}{2}-\frac{\xi_R-\xi_{\rm cc}}{2}R+(\xi_R-\tfrac{1}{2})H^2-\tfrac{1}{4}\dot H\right]\right]. \tag{2.38}$$

As expected, the introduction of a cutoff breaks the covariance of the formalism, resulting in a $\langle T_{\mu\nu}\rangle_{\rm sub}$ that cannot be written solely in terms of covariantly conserved geometrical tensors. On the other hand, we recognize that the divergent integrals in (2.37) and (2.38) vanish when evaluated in dimensional regularization [19]. Consequently, they are a product of our noncovariant formalism and we shall simply drop them.

Furthermore, in order to be consistent with the observed vanishing cosmological constant, we subtract $V_{\rm eff}(\varphi_{\rm min})g_{\mu\nu}$ from $\langle T_{\mu\nu}\rangle$, where $V_{\rm eff}(\varphi_{\rm min})$ is the value of the Gaussian effective potential at its minimum in Minkowski space-time. With these steps, we arrive at the following expressions for $\langle T_{00}\rangle_{\rm ren}$ and $\langle T_\mu^\mu\rangle_{\rm ren}$:

$$\begin{aligned}\langle T_{00}\rangle_{\rm ren}=&\frac{\pi^2}{2a^4}-\frac{\lambda_R}{12}\varphi^4+4a^{-2}\xi_R H\varphi\pi-\xi_R R_{00}\varphi^2-\frac{1}{2\lambda_R}[m_\delta^2(t)-\mu_R^2-(\xi_R-\xi_{\rm cc})R]^2+\tfrac{1}{2}[m_\delta^2(t)+\xi_{\rm cc}]\varphi^2\\&+\int_{\rm k}\left[\left[\frac{\dot G^2}{8G}+\tfrac{1}{2}m_\delta^2(t)G+\tfrac{1}{2}\xi_{\rm cc}RG-\xi_R R_{00}G+2\xi_R H\dot G\right]\left[\frac{1+\delta}{1-\delta}\right]^{1/2}\right.\\&\left.+\frac{1}{2ak}[\tfrac{1}{2}m_\delta^2(t)+(\xi_R-\xi_{\rm cc})(4H^2+2\dot H]\right]\\&+\int_{\rm k}\left[\left[\frac{1}{8a^4G}+\frac{k^2G}{2a^2}\right]\left[\frac{1+\delta}{1-\delta}\right]^{1/2}-\frac{k}{2a^3}\right]-\Lambda_c\ ,\end{aligned} \tag{2.39a}$$

$$\begin{aligned}\langle T_\mu^\mu\rangle_{\rm ren}=&4(\xi_R-\xi_{\rm cc})\frac{\pi^2}{a^4}+\lambda\left[\frac{4\xi_R}{3}-\frac{1}{4}\right]\varphi^4+(\tfrac{3}{2}-4\xi_R)[m_\delta^2(t)+\xi_{\rm cc}R]\varphi^2-\xi_R R\varphi-\frac{3}{2\lambda}[m_\delta^2(t)-\mu_R^2-(\xi_R-\xi_{\rm cc})R]^2\\&+4(\xi_R-\xi_{\rm cc})\int_{\rm k}\left[\left[\frac{1}{4a^4G}+\frac{\dot G^2}{4G}-\frac{k^2}{a^2}G\right]\left[\frac{1+\delta}{1-\delta}\right]^{1/2}-\frac{1}{8ak}[4m_\delta^2(t)+H^2]\right]-3\Lambda_c\ ,\end{aligned} \tag{2.39b}$$

where $\Lambda_c=V_{\rm eff}(\varphi_{\rm min})$ is given in the Appendix. Our $\langle T_{\mu\nu}\rangle_{\rm ren}$ satisfies the covariant conservation law

$$\nabla_\mu\langle T^{\mu\nu}\rangle_{\rm ren}=0\ . \tag{2.40}$$

III. DESCRIPTION OF THE CODE

In this article we solve the coupled differential Eqs. (2.23) with $\langle T_{00}\rangle$ replaced by $\langle T_{00}\rangle_{\rm ren}$. In principle our task is simple: the time evolution of the equations of motion is obtained by using a fifth-order Runge-Kutta method. However, we must be careful when choosing the initial condition since it must satisfy (2.31) and (2.32)—that is, $m_\delta^2(t_0)$ and $G_\delta(k,t_0)$ must be determined self-consistently. Furthermore, the Ricci scalar $R(=16\pi G_N T_\mu^\mu)$ and the Hubble constant $H[=\sqrt{8\pi G_N(\langle T_{00}\rangle_{\rm ren}+\langle T_{00}\rangle_{\rm rad})}]$ also depend on $m_\delta^2(t_0)$ and $G_\delta(k,t_0)$. Therefore, we must also evaluate H and R self-consistently. In our code, this is achieved by choosing a functional dependence of $G_\delta(k,t_0)$ on $m_\delta^2(t_0)$ given by (2.32) and then solving Eqs. (2.31) and (2.33) for $H(t_0)$, $m_\delta^2(t_0)$, and $R(t_0)$.

The expressions for $m_\delta^2(t)$, $\langle T_\mu^\mu\rangle_{\rm ren}$, and $\langle T_{00}\rangle_{\rm ren}$ involve momentum integrations, which are performed by introducing a cutoff Λ and using the Gauss method. Those integrals are Λ independent provided that Λ is large enough to allow $G(k,t)$ to approach its asymptotic limit (2.27) with $m^2(t)$ substituted by $m_\delta^2(t)$. In order to find out which Λ was needed, we evaluated $m_\delta^2(t_0)$, $\langle T_\mu^\mu\rangle_{\rm ren}(t_0)$, and $\langle T_{00}\rangle_{\rm ren}(t_0)$ using different Λ's. For the set of parameters used in this work, we concluded that a good choice is $\Lambda=M_P(=1/G_N)$, where M_P is the Planck mass. However, for any given value of Λ, it is possible that Λ stops being large enough after some time since the asymptotic form of $G(k,t)$ in (2.27) is time dependent. This occurs roughly for $\Lambda^2\le a^2(t)|m_\delta^2(t)|$. In order to verify that our results are reliable for all times, we follow the time evolution of $a(t)G_\delta(\Lambda,t)$, which should remain constant if the cutoff Λ is working well.

Since we ignore couplings between the inflation-driving scalar field and the other degrees of freedom (i.e., the thermal bath), (2.33) yields two separate conservation laws for the stress-energy tensor: one for the thermal bath ($\nabla_\mu\langle T^{\mu\nu}\rangle_{\rm rad}=0$) and another for the scalar field ($\nabla_\mu\langle T^{\mu\nu}\rangle_{\rm ren}=0$). In our code we used this last conservation law to monitor the time integration of the differential equations; more specifically, we evaluated

$$J\equiv\frac{\nabla_\mu\langle T^{\mu 0}\rangle_{\rm ren}}{\langle T^{00}\rangle_{\rm ren}}\times\text{time step}\ , \tag{3.1}$$

and checked that it was indeed always small, indicating that our calculations are reliable.

To estimate the roundoff errors further tests were carried out by evolving the system forward and backward in time. The difference between the initial state $G_\delta(k,t_0)$ and the one obtained after running forward and backward in time was negligibly small for most of the Fourier modes. We also tested the time integration of (2.33) by taking the scalar field contribution $\langle T^{00}\rangle_{\rm ren}\equiv 0$ and then solving for $a(t)$. In this case, we obtained the expected behavior $H=2/3t$.

IV. NUMERICAL RESULTS

In this section we shall present our numerical analysis, in which the quantum dynamics of the scalar field and the time evolution of the Universe have been studied self-consistently through the coupled Einstein-matter equations. We show whether and how inflation sets in under various initial conditions and also study how dynamics depends on the values of the parameters in the model: μ_R^2,λ_R, and ξ_R.

Initial conditions of the scalar field are given by specifying the values of the variational parameters $\varphi(t_0),\pi(t_0),G_\delta(k,t_0),\dot G_\delta(k,t_0)$ and $\delta(k)$, which define the Gaussian density matrix at an initial time t_0. Because of the symmetry $\Phi\rightarrow-\Phi$ in the Hamiltonian, different dynamics arise depending on whether or not the initial condition possesses this symmetry; if $\varphi(t_0)=\pi(t_0)=0$, then $\varphi(t)=\pi(t)=0$ for all $t>t_0$ due to the symmetry and if either $\varphi(t_0)\neq 0$ or $\pi(t_0)\neq 0$, then the system no longer has the symmetry, and both $\varphi(t)\neq 0$ and $\pi(t)\neq 0$ for $t>t_0$. For simplicity, we consider initial configurations with $\pi(t_0)=0$, so that the symmetry is present or absent in the system depending on whether $\varphi(t_0)$ is vanishing or nonvanishing. We shall consider initial states characterized by $\varphi(t_0)=0,\varphi(t_0)\ll\varphi_{\rm min},\varphi(t_0)\gg\varphi_{\rm min}$, and $\varphi(t_0)\approx\varphi_{\rm min}$, where $\varphi_{\rm min}$ is the location of the minimum of the effective potential in Minkowski space-time.

We parametrize $G_\delta(k,t_0)$ as in (2.25),

$$G_\delta(k,t_0)=G(k,t_0)\sqrt{1-\delta^2(k)} \tag{4.1a}$$

with

$$\dot G_\delta(k,t_0)=0 \tag{4.1b}$$

and take $G(k,t_0)$ to be one of the simplest forms which allows the system to be renormalized by the prescription (2.29). For all values of $\varphi(t_0)$ and for both pure and mixed states we have chosen

$$G(k,t_0)=\begin{cases} G_>(k,t_0)=\dfrac{1}{2a(t_0)k}-\dfrac{m_\delta^2(t_0)a^2(t_0)}{4k^3} & \text{for } k>\dfrac{\Lambda}{50}, \quad (4.2a)\\ G_<(k,t_0)=\dfrac{k+\epsilon}{\theta^2} & \text{for } k<\dfrac{\Lambda}{50}\ . \quad (4.2b)\end{cases}$$

Equation (4.2) contains several mass scales: Λ is the cutoff used in the numerical evaluation of the momentum integral, θ takes care of the correct dimensionality of $G_<(k,t_0)$ and ϵ is introduced to avoid infrared divergences in the equation of motion. Their magnitudes are chosen as $\Lambda=M_P$ and $\theta=10^{-2}M_P$ and $\epsilon=10^{-4}M_P$, where M_P is taken to be $M_P=100$ in the numerical calculation. The parameter $m_\delta^2(t_0)$ in $G_>(k,t_0)$ is a self-consistently determined initial mass.

We recall that the vacuum solution for large k modes ($k\gg aH$) is given by (2.27), where m_δ^2 is evaluated at $\varphi=\varphi_{\rm min}$ and $\delta(k)=0$. Therefore, a pure state described by (4.2) may be regarded as excitations relative to the vacuum, arising from $\varphi(t_0)\neq\varphi_{\rm min}$ and also from the fact that, for $k\lesssim aH$, $G_>(k,t_0)$ and $G_<(k,t_0)$ are different from the complete vacuum solution.

For mixed states where $\delta(k)\neq 0$, we must specify the form of $\delta(k)$. First, let us consider a thermal equilibrium initial configuration, which is the most interesting and representative among mixed states. $G_\delta(k,t_0)$ and $\delta(k)$ for a Boltzmann distribution at $T(t_0)$ may be obtained in the Gaussian approximation; however, since they are not in a closed form it is difficult to handle them as initial data. We shall instead construct a mixed state whose form resembles the thermal equilibrium solution for a free field in Minkowski space-time, which is given by

$$G(k)=\frac{1}{2\omega},\quad \omega\equiv\sqrt{k^2+\mu^2}\ , \tag{4.3a}$$

$$\delta^{-1}(k)=\cosh\frac{\omega}{T}\ . \tag{4.3b}$$

In the initial configuration $G(k,t_0)$ of (4.2) $G_>(k,t_0)$ for $k^2\gg m_\delta^2(t_0)a^2(t_0)$ is of the form (4.3a) up to $O(1/k^3)$, with ω replaced by an effective frequency

$$\omega_{\rm eff}(t_0)\equiv\sqrt{k^2+m_\delta^2(t_0)a^2(t_0)}\ . \tag{4.4}$$

Therefore, as a mixed initial state which can mimic a thermal equilibrium at $T(t_0)$, we shall take $G(k,t_0)$ in (4.2) and $\delta(k)$ given by

$$\delta^{-1}(k)=\cosh\frac{\omega_{\rm eff}(t_0)}{T(t_0)}\ . \tag{4.5}$$

In thermal equilibrium, $m_\delta^2(t_0)$ is evaluated at $\varphi(t_0)=0$ since the symmetry $\Phi\rightarrow-\Phi$ is expected to be restored. For the large momentum modes, $k\gg aH$, the above initial configuration is in fact a good approximation to the thermal equilibrium solution in the Gaussian approximation.

For more general mixed initial states we shall consider configurations with nonvanishing $\varphi(t_0)$, but with $G(k,t_0)$ and $\delta(k)$ still given by (4.2) and (4.5), since they can pro-

vide the effect of mixing.

The initial condition for the environmental thermal bath is given by the initial temperature $T(t_0)$, which then fixes the initial time. We have assumed the number of massless degrees of freedom in the thermal bath to be

$$g_B + \tfrac{3}{4} g_F = 200 \ .$$

Moreover, we have chosen our initial conditions and the values of the parameters μ_R^2, λ_R, and ξ_R such that initially the Universe is always radiation dominated and consequently the onset of inflation can be observed if it occurs.

In the Gaussian approximation we employ, all information about the behavior of quantum fluctuations is contained in the expectation value $\langle \Phi^2(\vec{x}) \rangle$. However, if one were to calculate $\langle \Phi^2(\vec{x}) \rangle$, one would find that it is divergent, due to the infinite quantum fluctuations in the field at a point. On the other hand, a measurable quantity with finite fluctuations can be defined in a manner that simulates the finite spatial resolution of a measuring device. For definiteness, we will use the smeared root-mean-square $\varphi_{\rm rms}^l(t)$ defined with a Gaussian weight function [10]:

$$\varphi_{\rm rms}^l(t) \equiv \left[\int_{\rm k} e^{-l^2 k^2} \frac{G_\delta(k,t)}{1-\delta(k)} \right]^{1/2} , \tag{4.6}$$

where l is the smearing length of our coarse-graining procedure. We shall choose l to be a fixed, time-independent constant since we are interested in following the evolution of an expanding region of space.

As mentioned earlier, if $\varphi(t_0)=0$ [with $\pi(t_0)=0$], $\varphi(t)=0$ for all t. Therefore, the expectation value of the quantum field cannot be a measure which tells us how much the system has evolved toward the minimum of the effective potential. Classically, the system will remain in its initial configuration. However, we find that dynamics is nontrivial quantum mechanically and $\varphi_{\rm rms}^l(t)$ exhibits a clear signal when the system starts to evolve toward the minimum [10].

To follow the time evolution of the Universe we keep track of the scale factor $a(t)$, the Hubble constant $H(t)$ and the Ricci scalar $R(t)$. The behavior of the scalar field is studied by examining $\varphi(t), \varphi_{\rm rms}^l(t)$, and the effective mass $m_\delta^2(t)$.

A. Initial configurations with $\varphi(t_0)=0$

We first analyze the quantum mechanics of the pure and mixed-state time evolution for an arbitrarily chosen set of values of μ_R^2, λ_R, and ξ_R and then study how the dynamics depends on μ_R^2, λ_R, and ξ_R by varying their values.

1. Pure state

The mass and coupling constants are chosen to be $\mu_R^2 = -10^{-6}, \lambda_R = 10^{-6}$, and $\xi_R = 0$ in the unit where $M_P = 100$. We have assumed that the environmental thermal bath is initially at temperature $T(t_0) = 10^{-2} M_P = 1$.

Our numerical results for this system are shown in Fig. 3. First, we find from Figs. 3(a)–3(c) that the Universe enters into de Sitter phase approximately at $t \simeq 4000$. Dynamics bringing about the onset of inflation may be understood from the behavior of the quantum fluctuations $\varphi_{\rm rms}^l(t)$ and the effective mass $m_\delta^2(t)$: Figure 3(d) shows that at early times $\varphi_{\rm rms}^l(t)$ decreases rapidly from its initial value, due to the fact that the fast expansion of the Universe redshifts away quantum fluctuations. This redshift can also be seen from the early time decrease in $m_\delta^2(t)$ in Fig. 3(e). At $t \approx 4000$, quantum fluctuations become negligible, leaving an approximately constant energy density, dominated by the cosmological constant Λ_c, and de Sitter expansion occurs with $H = \sqrt{8\pi G_N \Lambda_c}$. (Onset of de Sitter expansion implies that radiation energy of the environmental thermal bath also becomes negligible at $t \lesssim 4000$.)

We further observe in these figures time evolution of the scalar field after the onset of inflation. Once quantum fluctuations die away and de Sitter expansion starts, the effective mass $m_\delta^2(t)$ in Eq. (2.31) becomes a constant

$$m_\delta^2(t) \simeq -|\mu_R^2| + (\xi_R - \tfrac{1}{8}) R \ , \tag{4.7}$$

due to the fact that the Ricci scalar in de Sitter space is constant. Moreover, for the chosen value $\xi_R = 0$, $m_\delta^2(t)$ is negative, providing an unstable upside-down harmonic oscillator for the low-momentum modes [10]. Consequently, low-momentum modes tend to grow opposing the redshifts due to expansion of the Universe [see Fig. 3(f)]. The effect of these growing low-momentum modes may be seen from the behavior of $\varphi_{\rm rms}^l(t)$ for $t > 4000$. We interpret this growth of $\varphi_{\rm rms}^l(t)$ as a signal that the system starts to evolve toward the minimum of the potential [10].

On the other hand, the growth of low-momentum modes does not affect the constant energy density significantly, at least during our numerical run, and inflation continues as shown in Figs. 3(a)–3(c). [If the parameters in the model are chosen such that $m_\delta^2(t)$ in (4.7) is a positive constant, the effective potential during de Sitter phase has a local minimum at $\varphi=0$ and there would be no growth of low-momentum modes. The system then would evolve to the true minimum, through quantum tunneling, which we do not consider in this article.]

The monitoring of the numerical process is done by analyzing the quantities $a(t) G_\delta(\Lambda, t)$ and J defined in (3.1). For $t > 10\,000$ our calculations are not reliable any longer since $a(t) G_\delta(\Lambda, t)$ starts to depart from its asymptotic form (2.27) as can be seen in Fig. 3(g), and the cutoff Λ must be increased. On the other hand, during the entire period of our numerical evaluation, the covariant conservation of the stress-energy tensor of the scalar field is satisfied better than one part in 10^8 [see Fig. 3(h)].

To understand the influence of ξ_R on the time evolution of the system we performed a run with the same parameters and initial condition of the previous one, but with $\xi_R = \frac{1}{8}$ ("conformal coupling"). As can be seen from Fig. 4, the effect of changing ξ_R is to modify the rate of growth of the fluctuations, since for $\xi_R > 0, m_\delta^2$ is less negative than its value for $\xi_R = 0$.

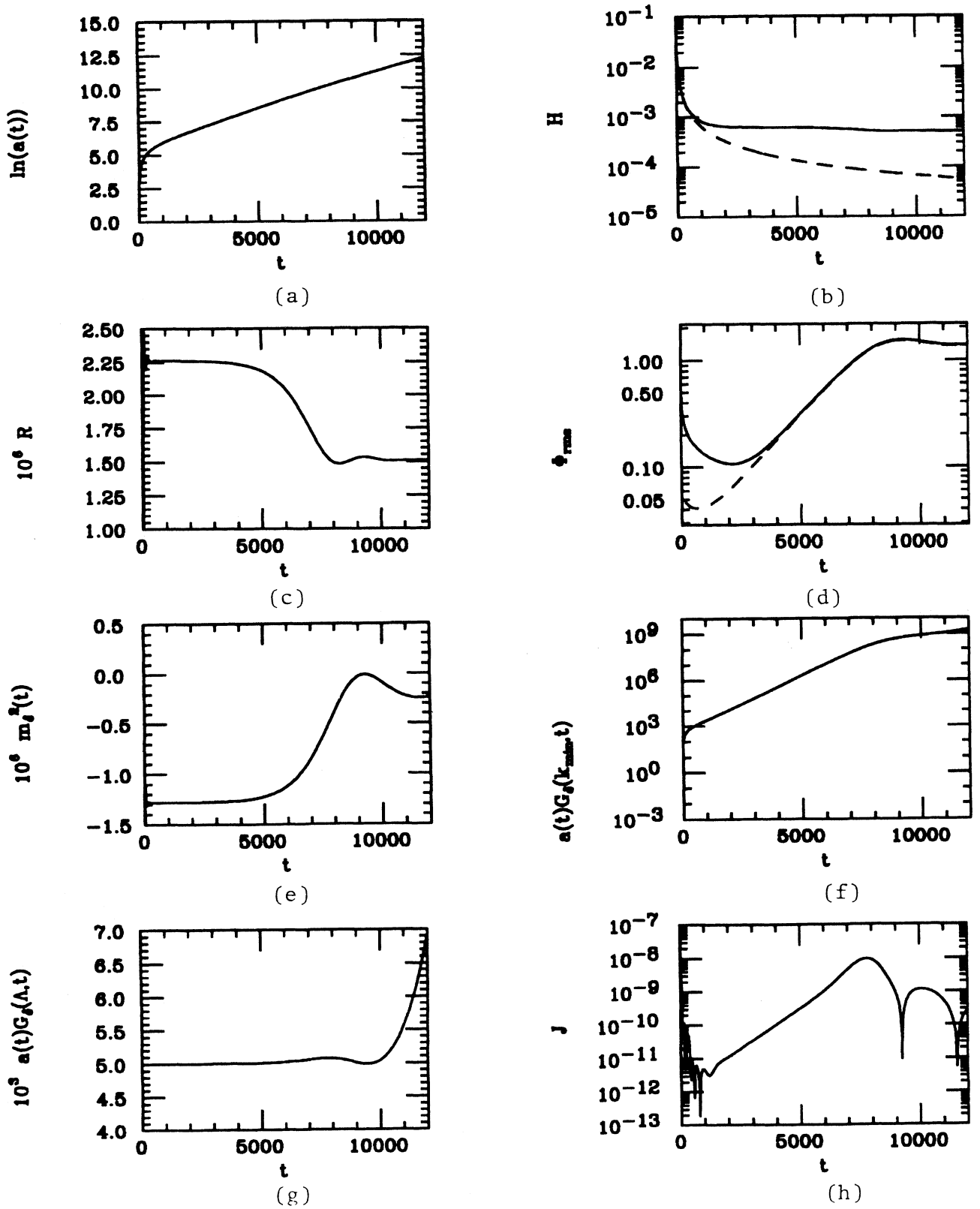

FIG. 3. Time evolution of the physical quantities for the run $\mu_R^2 = -10^{-6}, \lambda_R = 10^{-6}, \xi_R = 0$, and $T(t_0) = 1$ for the pure state with $\varphi(t_0) = 0$. (a) Scale factor $a(t)$. (b) Hubble constant $H(t)$ obtained in our calculation (solid line) and $H(t)$ in a radiation-dominated universe (dashed line). (c) Ricci scalar $R(t)$. (d) $\varphi_{\rm rms}^{l=1}(t)$ (dashed line) and $\varphi_{\rm rms}^{l=0.01}(t)$ (solid line). (e) Effective mass $m_\delta^2(t)$. (f) Evolution of the lowest momentum mode used $[a(t)G_\delta(k_{\rm min},t)]$. (g) Evolution of the largest momentum mode used $[a(t)G_\delta(\Lambda,t)]$. (h) Conservation law J.

2. *Mixed state: Initial thermal equilibrium*

We have studied time evolution of an initial state with $\varphi(t_0)=\pi(t_0)=0, G_\delta(k,t_0)$ and $\delta(k)$ given by (4.1), (4.2), and (4.5). We assume that the scalar field is in thermal equilibrium with itself and environment at temperature $T(t_0)=1.0$. Values of the parameters in the model are $\mu_R^2=10^{-6}, \lambda_R=1$, and $\xi_R=0$.

The result of our numerical run is shown in Fig. 5. One can see that this figure is similar to that of pure state in Fig. 3: Again, the quantum fluctuations $\varphi^l_{\rm rms}(t)$ decreases from a large initial value to a value much smaller than $\varphi_{\rm min}$ and inflation occurs due to the same physics.

To show the effect of mixture, we have given in Fig. 6 closer comparisons of the time evolution of the pure and mixed states by taking the same set of parameters $[\mu_R^2=-10^{-6}, \lambda_R=10^{-6}, \xi_R=0$, and $T(t_0)=1]$ for both cases: The small difference is due to the fact that fluctuations in a mixed state are enhanced by a factor $\sqrt{(1+\delta)/(1-\delta)}$, coming from the relations (4.1a) and (4.6).

3. *Dependence of dynamics on μ_R^2, λ_R, and ξ_R*

The question of how dynamics depend on the parameters μ_R^2, λ_R, and ξ_R has been studied by considering only the pure-state initial configuration where $\varphi(t_0)=\pi(t_0)=0$ and $G_\delta(k,t_0)$ given by (4.1) and (4.2) with $\delta(k)=0$ and the initial environment temperature $T(t_0)=1$. The ranges of the parameters we have considered are $\mu_R^2=-10^{-2}\sim-10^{-6}, \lambda_R=1\sim10^{-6}$, and for ξ_R we have taken two values: 0 and $\frac{1}{8}$. Figure 7 summarizes our results: we have observed inflation for all cases. The runs that yield a de Sitter period are indicated with I and the runs marked by Λ are the cases in which de Sitter expansion occurs but the numerical results are not reliable due to the fact that the cutoff Λ used was not large enough.

From a detailed numerical analysis we have found the following general features of the dependence of dynamics on μ_R^2, λ_R, and ξ_R. First, if their values are such that they produce a larger cosmological constant, inflation sets in at earlier time since the energy density becomes dominated by the cosmological constant more quickly as the quantum fluctuations redshift away. Once de Sitter expansion sets in, dynamics is governed by the value of the effective mass $m_\delta^2(t)$, which causes the growth of low-momentum modes: if the values of μ_R^2 and ξ_R are such that the value of $m_\delta^2(t)$ in (4.7) is a large negative number $\varphi^l_{\rm rms}(t)$ grows fast and the system evolves toward the minimum of the effective potential quickly. Clearly, this is not a desirable condition for the new inflationary

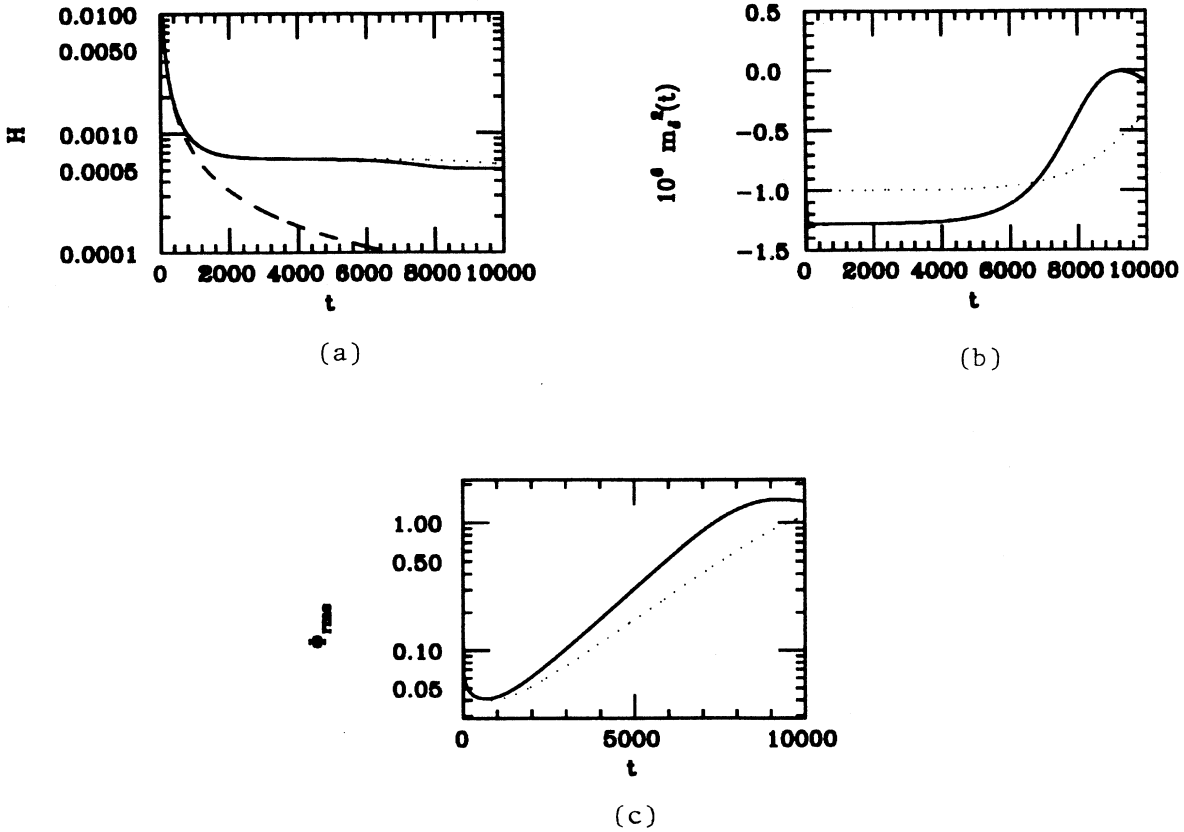

FIG. 4. Comparison between $\xi_R=0$ and $\xi_R=\frac{1}{8}$ in the time evolution of the pure initial state with $\varphi(t_0)=0, \lambda_R=10^{-6}, \mu_R^2=-10^{-6}, T(t_0)=1$. The solid line stands for $\xi_R=0$, while the dotted one for $\xi_R=\frac{1}{8}$. (a) Hubble constant H (the dashed line indicates the radiation-dominated universe); (b) $m_\delta^2(t)$; (c) $\varphi^{l=1}_{\rm min}(t)$.

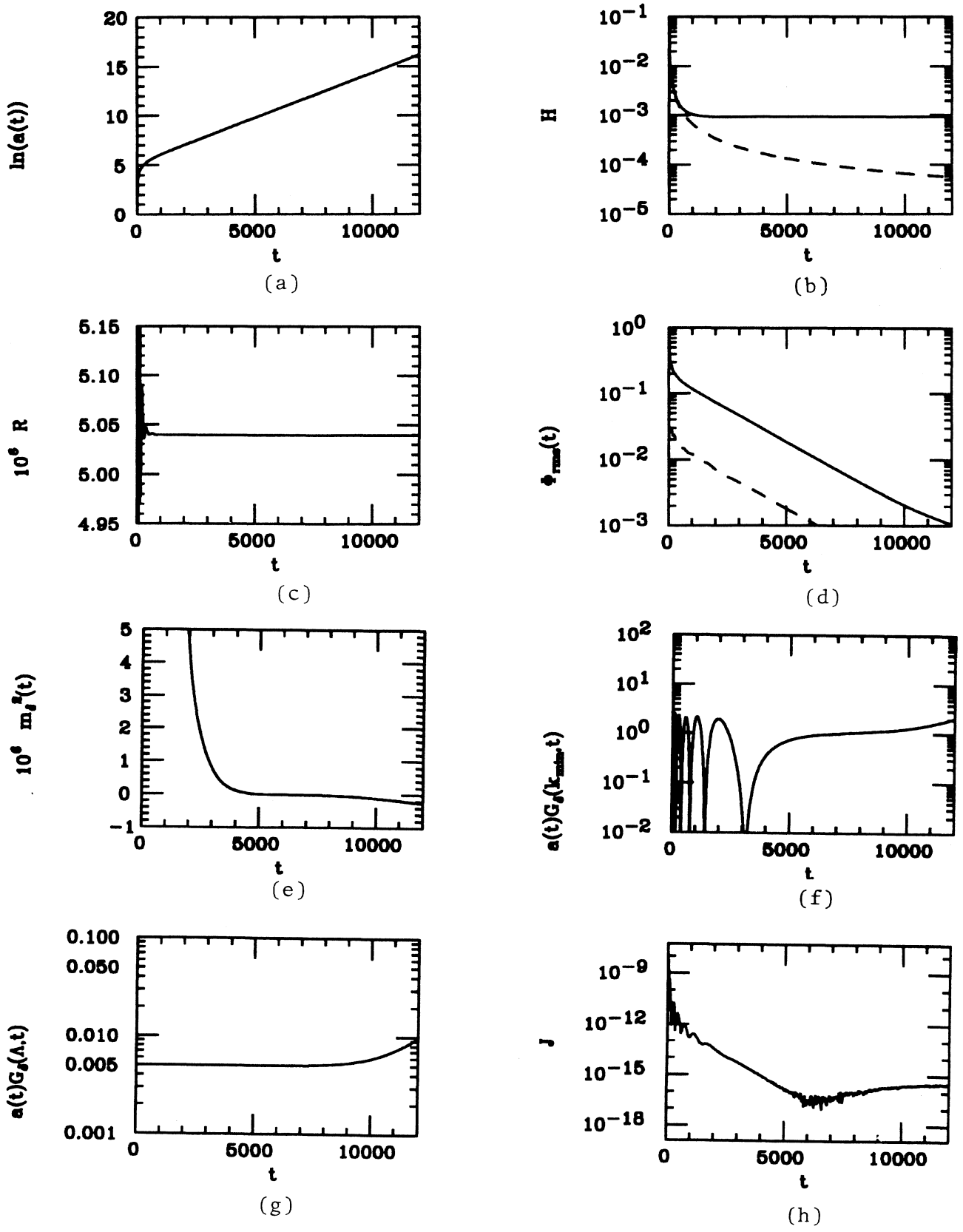

FIG. 5. Time evolution of the physical quantities as presented in Fig. 3 for the run $\mu_R^2=10^{-6}$, $\lambda_R=1$, $\xi_R=0$, and $T(t_0)=1$ for the mixed state. In this case $\varphi_{\rm rms}^{l=1}(t_0)=0.46$ and $\varphi_{\rm min}=0.138$.

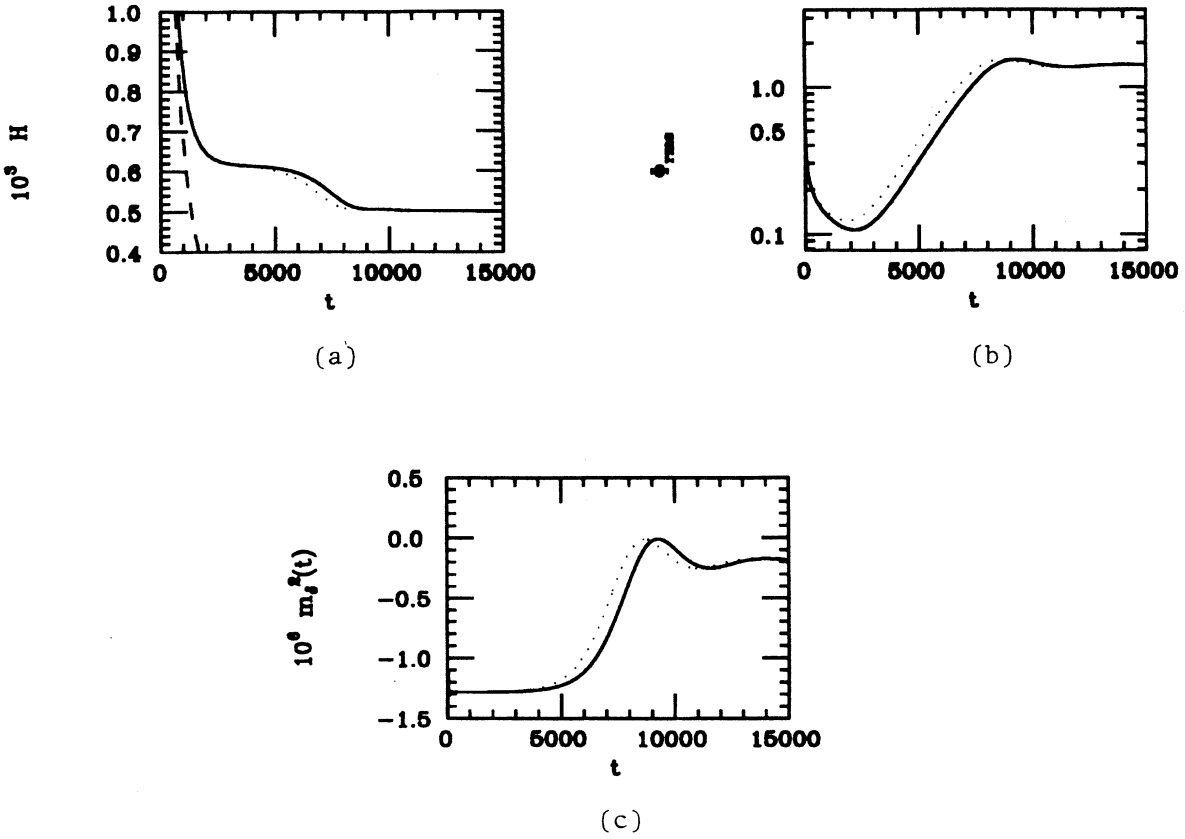

FIG. 6. Comparison of the time evolution between the pure state (solid line) and the mixed state (dotted line) for the case $\mu_R^2 = -10^{-6}, \lambda_R = 10^{-6}, \xi_R = 0$, and $T(t_0) = 1$. (a) Hubble constant $H(t)$ (dashed line indicated radiation-dominated universe). (b) $\varphi_{\rm rms}^{I=0.01}(t)$. (c) $m_\delta^2(t)$.

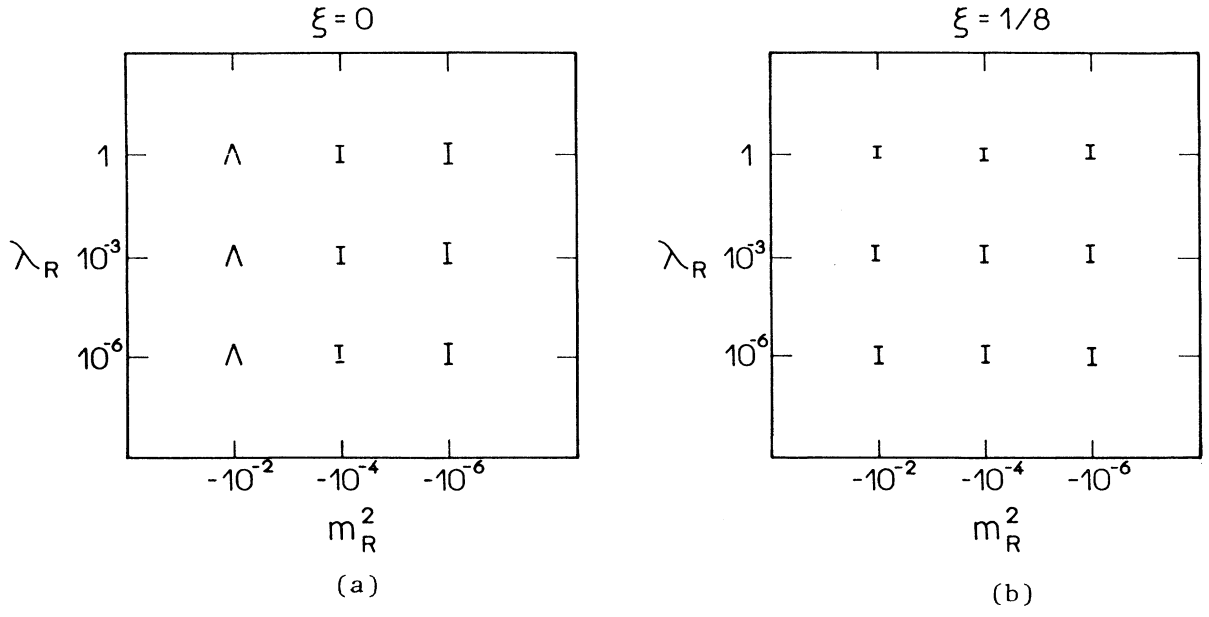

FIG. 7. Summary of the onset of inflation for various values of μ_R^2, λ_R, and ξ_R: For all cases de Sitter expansion has been observed. I indicates the numerical results which are reliable and Λ indicates the ones which are not reliable, but require larger cutoff.

scenario, which relies on a slow-rollover transition. Our numerical analysis concerns, however, only the early evolution of $\varphi^l_{\rm rms}(t)$. According to Ref. [10], which analyzes the quantum mechanics of slow-rollover transition in a linearized model, the late-time behavior of $\varphi^l_{\rm rms}(t)$ may be accurately described by the classical equation of motion, and therefore one expects that the value of λ_R controls the rate of growth as $\varphi^l_{\rm rms}(t)$ becomes large.

B. Initial configurations with nonvanishing $\varphi(t_0)$

When an initial state has a nonvanishing $\varphi(t_0)$, time evolution of $\varphi(t)$ for $t>t_0$ is nontrivial and it can be a measure of how the system has evolved toward the minimum of the effective potential. We have studied the evolution of initial states characterized by $\varphi(t_0)\ll\varphi_{\rm min}$ and $\varphi(t_0)\gg\varphi_{\rm min}$, for which one expects the dynamics to be very similar to the classical description of the "new" and "chaotic" inflationary scenarios, respectively. We have also considered an initial state with $\varphi(t_0)$, which is of the order of $\varphi_{\rm min}$ in magnitude. For all cases, we shall present in detail the time evolution of pure states only where $G_\delta(k,t_0)$ is given by (4.1) and (4.2) with $\delta(k)=0$, since we have found that introducing the mixing parameter (4.5) does not change the dynamics significantly. However, we shall make some comparisons between pure and mixed states.

1. *Initial configurations with* $\varphi(t_0)\ll\varphi_{\rm min}$

We consider a pure state with $\varphi(t_0)=10^{-6}\varphi_{\rm min}$, where $\varphi_{\rm min}=2.45$ for $\mu_R^2=-10^{-6}$, $\lambda_R=10^{-6}$, and $\xi_R=0$. The initial temperature for the environmental thermal bath is $T(t_0)=1$. Time evolution of the various quantities are shown in Fig. 8. At $t\simeq 3000$ the system enters into de Sitter phase due to the fact that the quantum fluctuations are redshifted away while $\varphi(t)$ stays close to zero resulting in an energy density dominated by the cosmological constant. As long as $\varphi(t)$ stays small, dynamics of the system are analogous to the case where $\varphi(t_0)=0$: once inflation sets in, and the fluctuations die out, the effective mass becomes

$$m_\delta^2(t)\simeq -|\mu_R^2|+(\xi_R-\tfrac{1}{8})R+\frac{\lambda_R}{2}\varphi^2(t)\ . \tag{4.8}$$

For small $\varphi(t)$, and for the chosen values of the parameters $m_\delta^2(t)$ is negative [see Fig. 8(e)] and therefore it provides an unstable upside-down potential for low-momentum modes of the fluctuations [Fig. 8(f)] and also for $\varphi(t)$. Consequently, both $\varphi^l_{\rm rms}(t)$ and $\varphi(t)$ grow as shown in Figs. 8(c) and 8(d). Figures 8(g) and 8(h) show that our numerical results are reliable for $t<10\,000$.

When we consider a mixed initial state by introducing $\delta(k)$ of (4.5), time evolution of the system does not change significantly, as can be seen from Fig. 9. In this figure we also show the effects of quantum fluctuations by comparing the time evolution in the Gaussian approximation with the classical evolution. Because of the fact that quantum fluctuations die away quickly in the early times by redshift, the early-time behaviors are almost the same. However, they are different for $t\gtrsim 5000$ due to the growth of low-momentum modes of quantum fluctuations.

2. *Initial configurations with* $\varphi(t_0)\gg\varphi_{\rm min}$

As mentioned earlier, one expects from a classical analysis that initial configurations with $\varphi(t_0)\gg\varphi_{\rm min}$ leads to de Sitter expansion as in "chaotic" inflationary scenario if the potential function is sufficiently flat. We have chosen $\mu_R^2=-10^{-12}$, $\lambda_R=10^{-12}$, and $\xi_R=0$ in order to have a flat potential. Our initial configuration is a pure state with $\varphi(t_0)=10\varphi_{\rm min}$ and $G_\delta(k,t_0)$ given by (4.1) and (4.2) where $\delta(k)=0$. The initial temperature of the environmental thermal bath is again $T(t_0)=1$. Time evolution of this system is shown in Fig. 10. As shown in Figs. 10(a) and 10(b) the system exhibits a de Sitter phase. Dynamics that lead to the de Sitter phase can be seen from Figs. 10(c)–10(h): While $\varphi(t)$ decreases very slowly, retaining an almost constant value during the entire period of our numerical run, $\varphi^l_{\rm rms}(t)$ gets redshifted away with a rate much faster than the rate of decrease of $\varphi(t)$, although the low-momentum modes increase steadily as shown in Fig. 10(f). Since the temperature of the environment also decreases by redshift, the resulting energy density of the system is approximately constant and therefore acts as a cosmological constant. Figures 10(g)–10(h) indicate that our numerical work is reliable during the entire period of the run. Once again we have verified that the time evolution does not change when we introduce a mixing by using $\delta(k)$ of the form (4.5).

3. *Initial configurations with* $\varphi(t_0)\simeq\varphi_{\rm min}$

We have also considered initial states, pure and mixed, with $\varphi(t_0)=2\varphi_{\rm min}$, $G_\delta(k,t_0)$ given by (4.1) and (4.2), and $T(t_0)=1$. As expected from classical equations of motion, we have found that $\varphi(t)$ oscillates around $\varphi_{\rm min}$, although quantum fluctuations somewhat change the evolution. Figure 11 shows the time evolution of $H(t)$ and $\varphi(t)$ for the cases of pure and mixed states when $\mu_R^2=-10^{-6}$, $\lambda_R=10^{-6}$, and $\xi_R=0$. We learn that de Sitter expansion never sets in and that pure and mixed-state time evolutions are again nearly the same.

V. CONCLUSIONS

In this article we have studied inflation dynamics during slow-rollover transitions, which occur under various initial configurations of the inflation-driving scalar field, concentrating on the two questions: How the onset of de Sitter expansion occurs and how the scalar field behaves during the early part of the slow-rollover transitions.

We have shown that de Sitter expansion sets in if the initial expectation value of the quantum field $\varphi(t_0)$ satisfies either $\varphi(t_0)\ll\varphi_{\rm min}$ or $\varphi(t_0)\gg\varphi_{\rm min}$ and at the same time if $\varphi(t)$ evolves very slowly in time. When these conditions are met, de Sitter expansion occurs regardless whether the scalar field is in a pure or a mixed state. The Universe enters into de Sitter phase due to the fact that both quantum fluctuations of the scalar field and the tem-

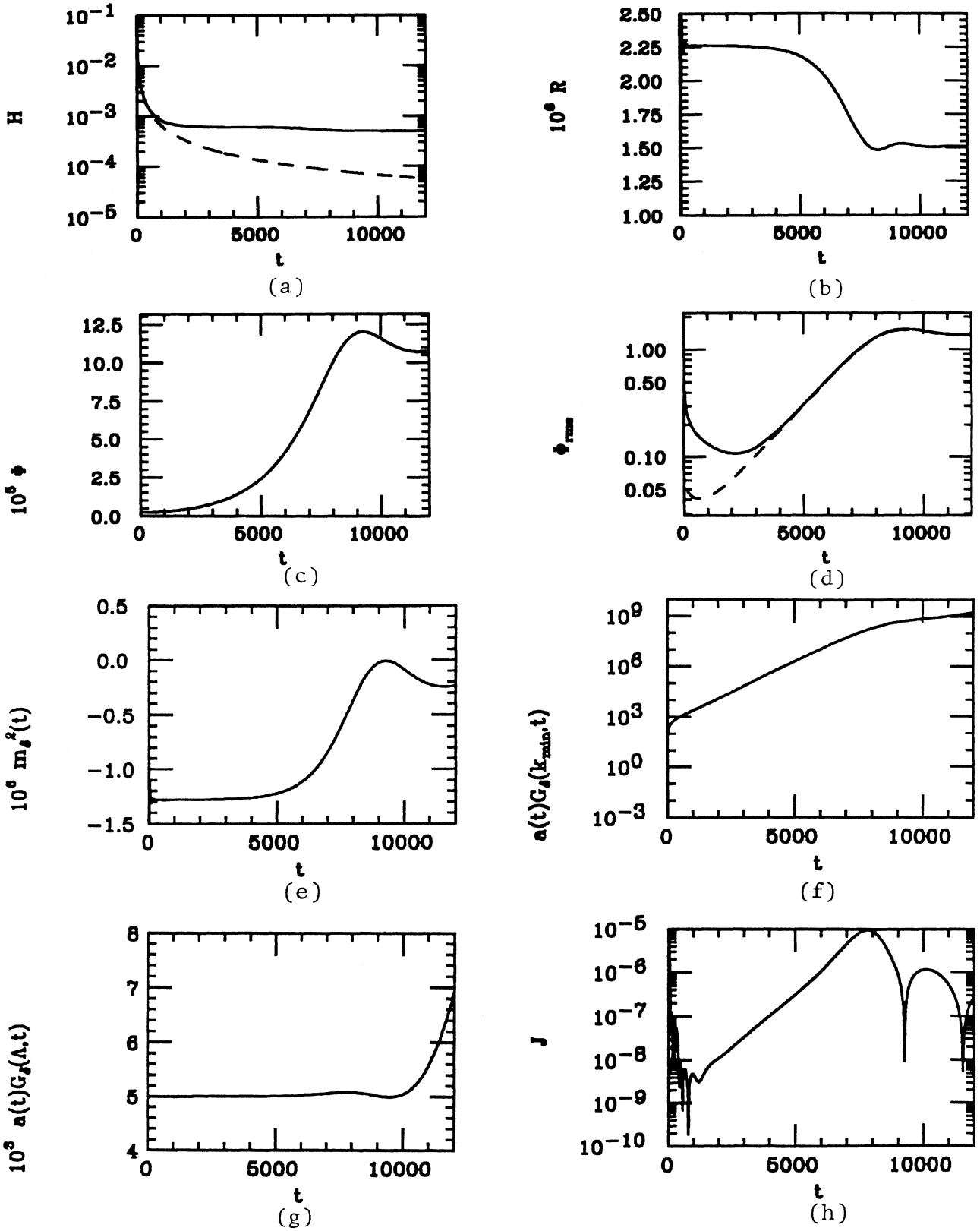

FIG. 8. Time evolution of the physical quantities for the run with $\mu_R^2=-10^{-6}, \lambda_R=10^{-6}, \xi_R=0$, and $T(t_0)=1$ for the pure state with $\varphi(t_0)=10^{-6}\varphi_{\min}$, where $\varphi_{\min}=2.45$. (a) Hubble constant $H(t)$ (dashed line indicates the radiation-dominated universe). (b) Ricci scalar $R(t)$. (c) $\varphi(t)$. (d) $\varphi_{\rm rms}^{l=1}(t)$ (dashed line) and $\varphi_{\rm rms}^{l=0.01}(t)$ (solid line). (e) $m_\delta^2(t)$. (f) Evolution of the lowest momentum mode $[a(t)G_\delta(k_{\min},t)]$. (g) Evolution of the largest momentum mode $[a(t)G_\delta(\Lambda,t)]$. (h) Conservation law J.

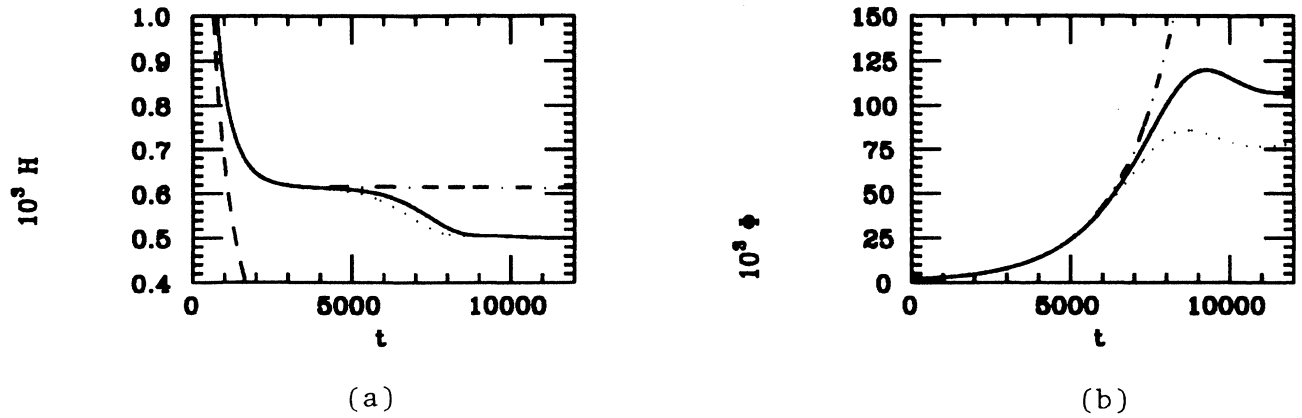

FIG. 9. Comparison of the pure (solid line), mixed (dotted line), and classical (dot-dashed line) evolutions for $\mu_R^2=-10^{-6}$, $\lambda_R=10^{-6}$, $\xi_R=0, T(t_0)=1$, and $\varphi(t_0)=10^{-6}\varphi_{\min}$, where $\varphi_{\min}=2.45$.

perature of the environmental thermal bath get redshifted away rapidly in early times, while $\varphi(t)$ evolves slowly [or remain constant in the case of $\varphi(t_0)=0$], leading to an approximately constant energy density.

For the thermal equilibrium initial configuration, which occurs in the new inflationary scenario, the behavior of $\varphi^l_{\rm rms}(t)$ is particularly important, since it plays the role of order parameter and therefore it determines when the system starts to evolve toward the minimum. We have shown that $\varphi^l_{\rm rms}(t)$ decreases rapidly during early times to a value much smaller than $\varphi_{\min}$ and then starts to grow.

It is instructive to compare our result for the case of thermal equilibrium initial configuration with some of the earlier calculations in the literature, for example, Refs. [10] and [11]. Our analysis may be considered as an extension of the work in Ref. [10] in several ways: First, in Ref. [10] quantum mechanics of the slow-rollover transition was studied in a linearized approximation, whereas we have studied effects of some of the nonlinearities using Gaussian approximation. Second, the linearized potential function used there is a "thermal equilibrium" zeroth-order approximation, while our method describes nonequilibrium time evolution. Finally, in Ref. [10] the background metric is assumed to be de Sitter space-time at all times and therefore the question of how the Universe approaches to de Sitter phase was not addressed, whereas in our analysis time evolution of Robertson–Walker metric has been determined self-consistently. The model considered of Ref. [10] consists of a single scalar field in de Sitter space-time with a potential function $V(\phi)=(\lambda/4)(\phi^2-\mu^2/\lambda)^2$. (This model does not contain environmental matter and radiation, which contributes to the total energy density. However, as can be seen in Fig. 12, the qualitative behavior of the scalar field is independent of the existence of the environment.) The scalar field is assumed to be in thermal equilibrium at early times and the potential is linearized to, at finite temperatures, $V_0(\varphi)=-\frac{1}{2}\{\mu^2-[\lambda T^2(t)/4]\}\phi^2$, where $T(t)$ redshifts as in our Eq. (2.8). $V_0(\phi)$ serves as a valid zeroth-order approximation in perturbation theory, while the scalar field remains in thermal equilibrium. The general qualitative behavior obtained in this linearized model is consistent with our result for the small values of λ considered ($\lambda\ll 1$). Namely, $\varphi^l_{\rm rms}(t)$ decreases to a value that is many orders of magnitude below $\varphi_{\min}=\mu/\sqrt{\lambda}$, and then starts to grow at a temperature well below T_c, indicating the existence of supercooling. The reason for the continued falling of $\varphi^l_{\rm rms}(t)$ in this model has been explained as follows: At temperatures $T\approx T_c$, $\varphi^l_{\rm rms}(t)$ is dominated by the momentum modes $k^2a^{-2}(t)\approx T^2\approx 4\mu^2/\lambda$. For $\lambda\ll 1$, the fact that $V_0(\phi)$ becomes unstable at $T<T_c$ is therefore irrelevant to these modes and they continue to get redshifted like a free field. This, on the other hand, suggests that for $\lambda\approx 1$ the dominant modes feel the unstable potential at $T\approx T_c$ and the falling of $\varphi^l_{\rm rms}(t)$ would presumably stop and $\varphi^l_{\rm rms}(t)$ would settle into $\varphi_{\min}$. However, this explanation for the falling of $\varphi^l_{\rm rms}(t)$ given in Ref. [10] comes from the fact that $V_0(\phi)$ is the zeroth-order "equilibrium" potential and therefore the dominant modes of $\varphi^l_{\rm rms}(t)$ turn out to be related to the critical temperature $T_c=2\mu/\sqrt{\lambda}$. If we were to apply the zeroth-order equilibrium potential in 2+1 dimensions, we expect that the continued falling to a value smaller than $\varphi_{\min}$ would occur only if $\mu^2\gg\lambda^2$. (In 2+1 dimensions λ is not dimensionless and moreover, the form of the finite temperature effective potential is different from that in 3+1 dimensions.) However, we find that, in our nonequilibrium calculation, the continued falling occurs for a wide range of λ even when $\lambda^2\ll\mu^2$. Moreover, the same phenomenon occurs for a pure state with $\varphi(t_0)=0$ for which the magnitude of the dominant modes of $\varphi^l_{\rm rms}(t)$ is irrelevant to the temperature. Our result implies that at early times, whether the system is initially in thermal equilibrium or not, $\varphi^l_{\rm rms}(t)$ is simply dominated by large k modes such that the negative curvature (4.7) is irrelevant to the dynamics for a

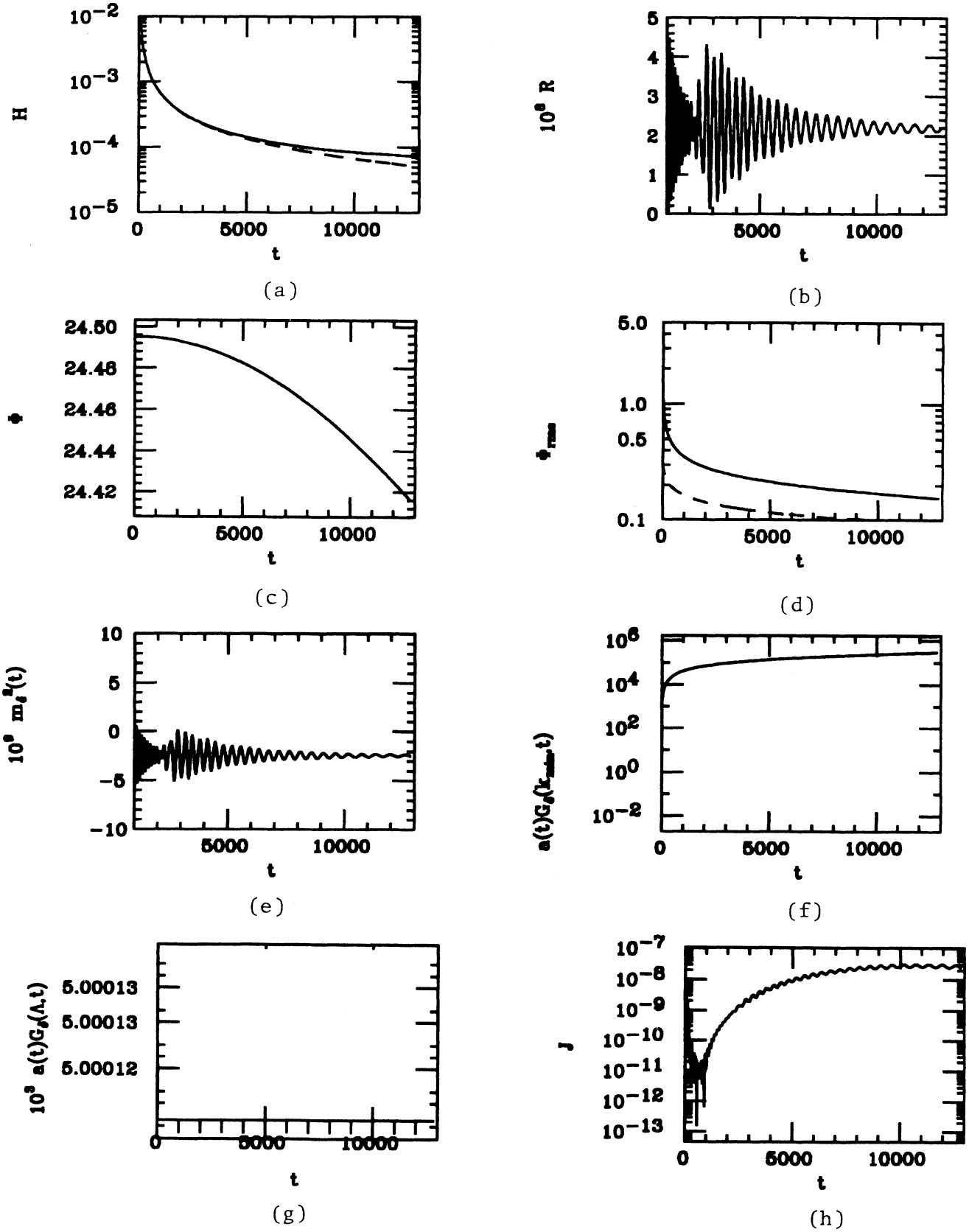

FIG. 10. Time evolution of the physical quantities for the pure state with $\varphi(t_0)=10\varphi_{\min}$ for $\mu_R^2=-10^{-12}$, $\lambda_R=10^{-12}$, $\xi_R=0$, and $T(t_0)=1$ as in Fig. 8.

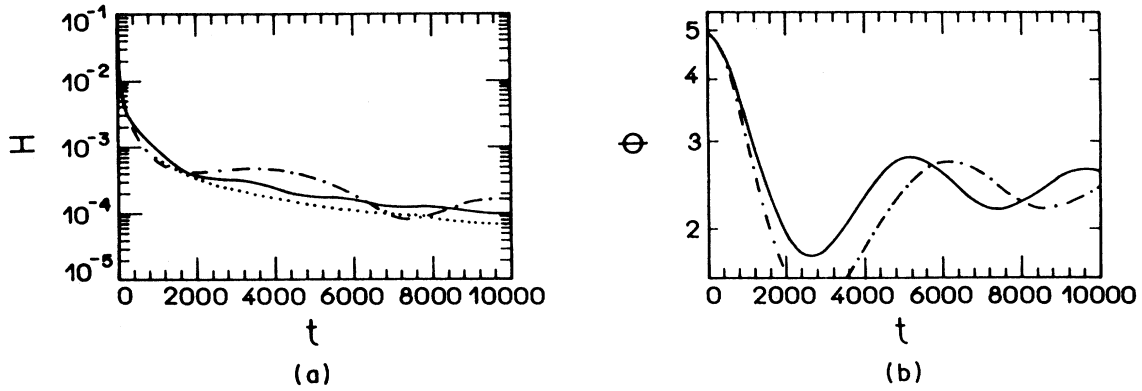

FIG. 11. Comparison of the time evolution of different initial conditions for $\mu_R^2=-10^{-6}$, $\lambda_R=10^{-6}$, and $\varphi(t_0)=2\varphi_{\min}$: pure state with $\xi_R=0$ (solid line); mixed state with $\xi_R=0$ (dashed line); pure state with $\xi_R=\frac{1}{8}$ (dot-dashed line). (a) $H(t)$, where the dotted line stands for the radiation-dominated universe; (b) $\varphi(t)$.

long time.

Next, we comment on the analysis of Ref. [11]. The model and approximation technique used in Ref. [11] are complementary to ours: Here inflation dynamics was studied in an O(N) model of scalar fields using the leading large-N approximation, and the behavior of the Robertson–Walker background metric has been determined self-consistently as in our analysis.

In large-N approximation the evolution equations of the correlation functions of each component field, $\langle\Phi_i(\mathbf{x},t)\Phi_i(\mathbf{y},t)\rangle$, $\langle\Phi_i(\mathbf{x},t)\Pi_i(\mathbf{y},t)\rangle$, and $\langle\Pi_i(\mathbf{x},t)\Pi_i(\mathbf{y},t)\rangle$ are closed. It is straightforward to show that the large-N equations are the same as our Gaussian variational equations for G,Σ, and δ using the relations in (2.22), except that the effective mass term in the large-N does not contain a $\frac{1}{2}$ factor multiplying λ due to different combinatorics in the Feynman diagrams:

$$m_N^2(t)=-\mu^2+\lambda\int\frac{d^3k}{(2\pi)^3}G(k,t)\left[\frac{1+\delta(k)}{1-\delta(k)}\right]^{1/2}. \quad (5.1)$$

(The subscript N denotes large-N approximation.) In spite of the fact that the two approximations are equivalent the results obtained in Ref. [11] are very different from ours. We believe that this difference in physics is due to the different techniques used in handling quantum-field-theoretic infinities.

Field theoretic infinities appear, in both approximations, in the correlation function

$$\langle\Phi^2(\mathbf{x},t)\rangle=\int\frac{d^3k}{(2\pi)^3}G(k,t)\left[\frac{1+\delta(k)}{1-\delta(k)}\right]^{1/2}. \quad (5.2)$$

As shown in this article, the infinities in $\langle\Phi^2(\mathbf{x},t)\rangle$ must be taken care of in two different ways: First, in the equation of motion, one must perform a consistent renormalization, which involve renormalization of λ, μ, and ξ in (3+1)-dimensional space-time. (ξ renormalization is necessary even when $\xi=0$ in the bare Lagrangian.) Similarly, the energy-momentum tensor must be renormalized in a covariant manner in the Einstein equation. Second,

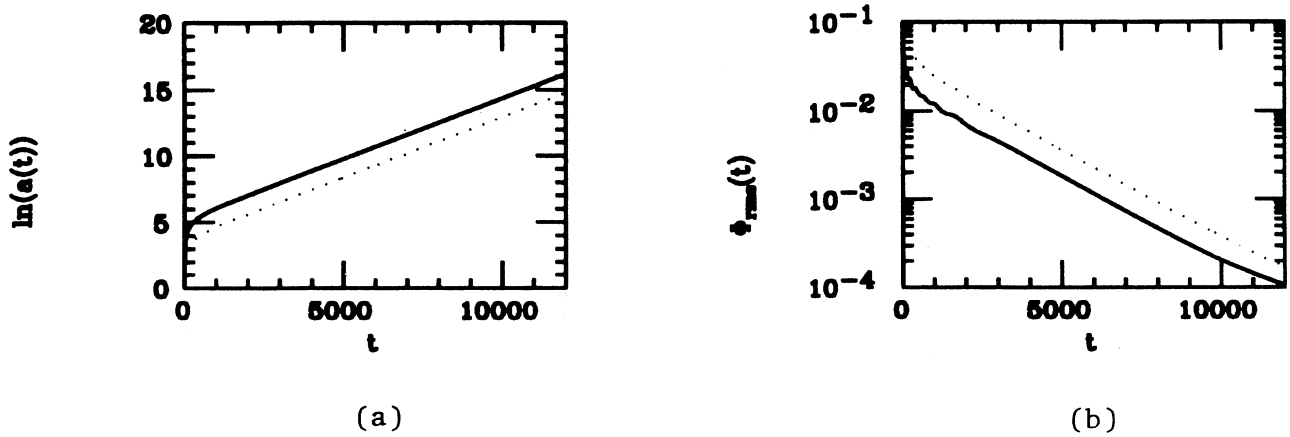

FIG. 12. Comparison of the time evolution shown in Fig. 5 (solid line), which includes the environment, and the same run without the environmental thermal bath (dotted line). In these runs $\varphi_{\min}=0.138$ and $\varphi_{\rm rms}^{l=1}(t_0=0)=1.63$ in both cases. (a) $\ln[a(t)]$; (b) $\varphi_{\rm rms}^{l=1}$.

when $\langle \Phi^2(\mathbf{x},t)\rangle$ is used as a short-range order parameter, the infinities are physically real and must be handled in such a way that the effects of quantum fluctuations are kept properly.

In Ref. [11], only the infinities in the initial state are removed by normal ordering; the approximate initial thermal equilibrium configuration is similar to ours before normal ordering:

$$\langle \Phi^2(\mathbf{x},t_0)\rangle = \int \frac{d^3k}{(2\pi)^3}\frac{1}{2\omega_N(k,t_0)}\left[1+\frac{2}{e^{\omega_N/T}-1}\right], \tag{5.3}$$

where $\omega_N^2(k,t_0)=(k^2a^{-2}+m_N^2)|_{t_0}$. By normal ordering, the vacuum fluctuations are then dropped, and the initial value of $\langle \phi^2(\mathbf{x},t_0)\rangle$ has been chosen as

$$\langle \Phi^2(\mathbf{x},t_0)\rangle = \int \frac{d^3k}{(2\pi)^3}\frac{1}{\omega_N(k,t_0)}\frac{1}{e^{\omega_N(k,t_0)/T}-1}\ . \tag{5.4}$$

Reference [11] claims that (at least in the large-N limit), if one regulates the initial conditions and then follows the subsequent dynamic evolution generated by the equation of motion, one generates no new singularities. On the contrary, we find that quadratic divergences are generated in the subsequent dynamic evolution, independently of the initial condition, and conventional renormalization of coupling constants and mass is necessary [19]. This then forces the initial state to be renormalized in the same manner. However, it is well known [13] that the renormalized large-N approximation in $3+1$ dimensions leads to difficulties and this is precisely the reason why we performed our analysis in $2+1$ dimensions, since Gaussian approximation possesses the same difficulties in higher dimensions. Moreover, the initial value of our order parameter obtained by smearing as in (4.6) is quite different from the initial value of the order parameter (5.4) taken in Ref. [11]. Taking (5.4) to describe thermal equilibrium properties on a classical level is presumably acceptable. However, in studying quantum evolution one cannot separate quantum fluctuations from thermal fluctuations.

In the results obtained in Ref. [11] $\langle \Phi^2(\mathbf{x},t)\rangle$ decreases from its initial value and directly settles to $\varphi^2_{\min}$, where $\varphi_{\min}$ is the location of the minimum of the tree-level potential. The continued falling of $\langle \Phi^2(\mathbf{x},t\rangle$ to a value much smaller than $\varphi_{\min}$ observed in the numerical results of ours and Ref. [10] does not occur and it is stated that "Indeed the 'ball rolling down the hill' advocated by a number of authors does not result in this model except that in the case where the system is prepared in a nonequilibrium initial state where the level of order parameter fluctuations are constrained to be much less than in the associated thermal state."

On the other hand, Fig. 12 indicates that the "ball rolling down the hill" picture occurs for the thermal equilibrium initial state, even when the environment is absent as in the model of Ref. [11]. We believe that such a different result is not due to effect of dimensionality.

In this article we have studied only the onset of the de Sitter phase and only the early-time behavior of the scalar field. We did not pursue our calculation for the late-time behavior of the system. This will determine the duration of de Sitter expansion, which puts constraints on inflationary model building. However, this problem is relevant only to the physical $(3+1)$-dimensional spacetime. We hope to return to this in the future when a calculational scheme appropriate to $3+1$ dimensions is available.

ACKNOWLEDGMENTS

This work was supported in part by funds provided by the U.S. Department of Energy (D.O.E.) under Contracts Nos. DE-AC02-86ER140284 and DE-AC0287ER40325B, as well as by the Conselho Nacional de Desenvolvimento Científico e Tecnológico (CNPq), Brazil and Fundação de Amparo a Pesquisa do Estado de São Paulo (FAPESP), Brazil.

APPENDIX

For completeness we record in this appendix the Gaussian effective potential. In general, the effective potential is given by

$$V_{\text{eff}}(\varphi)=\min_{|\Psi\rangle}\langle \Psi|H|\Psi\rangle\ , \tag{A1}$$

where $|\Psi\rangle$ satisfy the constraint

$$\langle \Psi|\Phi|\Psi\rangle=\varphi\ . \tag{A2}$$

The Gaussian effective potential is the result of (A1) when we restrict the states $|\Psi\rangle$ to be Gaussian. For $a=1,\dot\varphi=0$, and $\dot G=0\langle T_{00}\rangle_{\text{ren}}$ in (2.34) is simply $\langle \Psi|H|\Psi\rangle$ in a Gaussian state. Therefore,

$$V_{\text{eff}}(\varphi)=\min_G\langle T_{00}\rangle_{\text{ren}}\ . \tag{A3}$$

Carrying out the minimization in (A3) yields that

$$G=\frac{1}{2\sqrt{\mathbf{k}^2+m^2}}\ , \tag{A4a}$$

where

$$m^2=\mu_R^2+\frac{\lambda_R}{2}\varphi^2+\frac{\lambda_R}{2}\int_{\mathbf{k}}\left[\frac{1}{2\sqrt{\mathbf{k}^2+m^2}}-\frac{1}{2|\mathbf{k}|}\right]. \tag{A4b}$$

Consequently, the renormalized Gaussian effective potential is given by

$$V_{\text{eff}}=\frac{m^4}{2\lambda_R}+\frac{m^3}{24\pi}-\frac{\mu_R^4}{2\lambda_R}-\frac{\lambda_R}{12}\varphi^4 \tag{A5a}$$

with

$$m=-\frac{\lambda_R}{16\pi}+\left[\left[\frac{\lambda_R}{16\pi}\right]^2+\mu_R^2+\frac{\lambda_R}{2}\varphi^2\right]^{1/2}. \tag{A5b}$$

The minimum $\varphi_{\min}$ of V_{eff} is located at

$$\varphi_{\min}=\frac{\sqrt{3\lambda_R}}{8\pi}\left[1+\left[1-\frac{128\pi^2\mu_R^2}{\lambda_R}\right]^{1/2}\right] \tag{A6}$$

for $\lambda_R\geq 128\pi^2\mu_R^2$. Otherwise $\varphi_{\min}=0$.

*Permanent address: Instituto de Física, Universidade de São Paulo, C.P. 20516, São Paulo 01498, Brazil.

[1] For a review, see L. Abbott and S.-Y. Pi, *Inflationary Cosmology* (World Scientific, Singapore, 1986).

[2] A. H. Guth, Phys. Rev. D **15**, 347 (1981); A. H. Guth and E. J. Weinberg, Nucl. Phys. **B212**, 321 (1983).

[3] A. D. Linde, Phys. Lett. **108B**, 389 (1982); A. Albrecht and P. J. Steinhardt, Phys. Rev. Lett. **48**, 1220 (1982).

[4] A. D. Linde, Phys. Lett. **128B**, 177 (1983).

[5] D. La and P. J. Steinhardt, Phys. Rev. Lett. **62**, 376 (1989).

[6] D. A. Kirzhnits and A. D. Linde, Phys. Lett. **42B**, 471 (1972); L. Dolan and R. Jackiw, Phys. Rev. D **9**, 3320 (1974); S. Weinberg, *ibid.* **9**, 3357 (1974).

[7] A. A. Starobinsky, Phys. Lett. **117B**, 175 (1982); A. H. Guth and S.-Y. Pi, Phys. Rev. Lett. **49**, 1110 (1982); J. M. Bardeen, P. J. Steinhardt, and M. S. Turner, Phys. Rev. D **28**, 679 (1983).

[8] Quantum-mechanical nonequilibrium dynamics in the context of the new inflationary model was first studied in a linearized approximation by J. M. Cornwall and R. Bruinsma, Phys. Rev. D **38**, 3144 (1988).

[9] See, for example, A. Albrecht and R. Brandenberger, Phys. Rev. D **31**, 1225 (1985); A. Albrecht, R. Brandenberger, and R. Matzner, *ibid.* **32**, 1280 (1985); **35**, 429 (1987); H. Kurki-Suonio, J. Centrella, R. Matzner, and J. Wilson, *ibid.* **35**, 435 (1987); R. Brandenberger, H. Feldman, and J. MacGibbon, *ibid.* **37**, 2071 (1988).

[10] A. H. Guth and S.-Y. Pi, Phys. Rev. D **32**, 1899 (1985).

[11] G. F. Mazenko, Phys. Rev. Lett. **54**, 2163 (1985); Phys. Rev. D **34**, 2223 (1986).

[12] O. Eboli, R. Jackiw, and S.-Y. Pi, Phys. Rev. D **37**, 3557 (1988).

[13] Many works treat this problem. See, for instance, S. Coleman, R. Jackiw, and H. D. Politzer, Phys. Rev. D **8**, 2491 (1974); or W. A. Bardeen and M. Moshe, *ibid.* **28**, 1372 (1983).

[14] For a review, see R. Jackiw, in *Field Theory and Particle Physics,* V. Jorge Andre Swieca Summer School, Campos do Jordâo, Brazil, 1989, edited by O. Eboli, M. Gomes, and A. Santoro (World Scientific, Singapore, 1990).

[15] P. A. M. Dirac, *Principles of Quantum Mechanics,* 4th ed., International Series of Monographs on Physics (Oxford University Press, Oxford, England, 1958), appendix; Proc. Cambridge Philos. Soc. **26**, 376 (1930).

[16] R. Balian and M. Vènèroni, Phys. Rev. Lett. **47**, 1353 (1981); **47**, 1765(E) (1981); Ann. Phys. (N.Y.) **164**, 334 (1985).

[17] R. Jackiw and A. Kerman, Phys. Lett. **71B**, 158 (1979).

[18] N. D. Birrell and P. C. W. Davies, *Quantum Fields in Curved Space* (Cambridge University Press, Cambridge, England, 1982).

[19] O. Eboli, S.-Y. Pi, and M. Samiullah, Ann. Phys. (N.Y.) **193**, 102 (1989).

[20] G.'t Hooft and M. Veltman, Nucl. Phys. **B44**, 189 (1972); C. G. Bollini and J. J. Giambiagi, Phys. Lett. **40B**, 566 (1972); J. F. Ashmore, Nuovo Cimento Lett. **4**, 289 (1972).

[21] The fact that the dynamics is governed by $m_\delta^2(t)$ rather than $m_\delta^2(t)+\xi_{cc}R$, which appears in (2.26a), can be seen more clearly if we write the equation of motion (2.26a) in terms of conformal variables $G_c(k,\eta)=aG(k,t)$, with $d\eta/dt=1/a(t)$:

$$\frac{\partial^2}{\partial\eta^2}G_c=\tfrac{1}{2}G_c^{-1}+\tfrac{1}{2}G_c^{-1}\left[\frac{\partial G_c}{\partial\eta}\right]^2-2(k^2+a^2m_\delta^2)G_c\ .$$